Tracing sources and fate of nitrate in multilayered karstic hydrogeological catchments using natural stable isotopic composition (δ15N-NO3– and δ18O-NO3–). Application to the Toulon karst system (Dordogne, France)

Guillaume Lorette, Mathieu Sebilo, Damien Buquet, Roland Lastennet, Alain Denis, Nicolas Peyraube, Veronique Charriere, Jean-Christophe Studer

Tracing sources and fate of nitrate in multilayered karstic hydrogeological catchments using natural stable isotopic composition ($\delta^{15}N_{-NO3^-}$ and $\delta^{18}O_{-NO3^-}$). Application to the Toulon karst system (Dordogne, France)

Guillaume LORETTE[1-2*], Mathieu SEBILO[3], Damien BUQUET[1], Roland LASTENNET[1], Alain DENIS[1], Nicolas PEYRAUBE[1], Veronique CHARRIERE[4], Jean-Christophe STUDER[5].

1 University of Bordeaux, I2M-GCE CNRS 5295, 33 405 Talence, France.
2 Syndicat Mixte des Eaux de la Dordogne, 24 430 Marsac sur l'Isle, France.
3 Sorbonne Université, CNRS, INRAE, IRD, UPD, UPEC, Institute of Ecology and Environmental Sciences – Paris, iEES, 75005 Paris, France.
4 Sorbonne Université, Département des Langues, 75005 Paris, France
5 SUEZ Eau France, Périgueux, France.

Corresponding author at: University of Bordeaux, I2M-GCE-CNRS 5295, 351 cours de la liberation 33405 Talence, Bât A11, France.
E-mail address: lorette.guillaume@gmail.com

Abstract

In groundwater management, the determination of the origins of nitrate (NO_3^-) endmember sources is the first step in improving the management over a hydrogeological catchment. The generally multiple source contamination by nitrate over the karst systems makes it difficult to identify the exact nitrate origins in surface water and groundwater.

This work aims to assess nitrate vulnerability of a karst system fed by several karst aquifers. The Toulon karst system offers the opportunity to study the relationships between two multilayered karst aquifers. It shows an increase in mean NO_3^- concentrations over decades. However, the origins of the NO_3^- remain unclear. Natural stable isotopic composition of NO_3^- ($\delta^{15}N_{-NO3^-}$ and $\delta^{18}O_{-NO3^-}$) measurements combined with concentrations were used to identify the origins of nitrogen causing this increase. This information was also integrated into the local hydrogeological situation to improve knowledge of the contamination of both confined and unconfined karst aquifers.

$\delta^{15}N_{-NO_3^-}$ and $\delta^{18}O_{-NO_3^-}$ in potential nitrate sources over the hydrogeological catchment were analysed in order to identify the range of values that can be measured in both rivers and groundwater. Over the Toulon Springs catchment, rivers are contaminated with nitrate coming from N synthetic fertilizer mineralized in agriculturalsoils. Most of the springs are also contaminated by this nitrate source, but some record an isotope composition of nitrate coming from sewage effluents. Toulon Springs are only contaminated with nitrate from N synthetic fertilizer mineralized in agricultural soils. Finally, from a hydrogeological point of view, the analysis of $\delta^{15}N_{-NO_3^-}$ and $\delta^{18}O_{-NO_3^-}$ values improves knowledge on the functioning of the study area and shows that the upper Jurassic karst confined aquifer has nitrate of the same origins (sources) as the upper Cretaceous unconfined aquifer. The results here highlight that the lower aquifer can be fed by the Upper Cretaceous unconfined aquifer, contrary to previous belief that the lower aquifer was confined.

From a more fundamental standpoint, this work provides a set of parameters adapted for karstic hydrogeological catchment. It lays the foundation for the use of isotope biogeochemistry as a powerful tool for understanding the recharge of drinking water catchments and beyond the efficient management of water quality at the scale of karstic hydrogeological catchment.

Keywords: nitrate, karst, multilayered aquifer, nitrate isotopes, hydrochemistry.

Highlights:

- Nitrate contents and isotopes are measured in a large multilayered karst aquifer
- Primary and secondary sources of nitrate are determined, at the local scale, using nitrate isotopes

- Origins of nitrate, over a karstic hydrogeological catchment, are assessed by nitrate isotopes
- The fate of nitrate in a karst aquifer is specified/ elucidated/ quantified/ combining isotopes and hydrogeological approaches

1. Introduction

Karst aquifers are one of the most important water supply sources worldwide. Approximately 20-25% of the world's population consumes water obtained from karst aquifers (Ford and Williams, 2007; Goldscheider et al. 2020). These aquifers are distinguished from porous aquifers by the high degree of heterogeneity that can be identified in both surface and underground environments (White, 1988; Bakalowicz, 2005). This heterogeneous characteristic implies a high flow rate into karst systems which could reach several hundred m h^{-1} (Mudarra et al. 2014; Marin et al. 2015). These unique hydrogeological characteristics make karst aquifers particularly vulnerable to surface contamination and difficult to manage (Stevanović, 2015, 2019).

Nitrate (NO_3^-) is the most persistent and mobile form of nitrogen in the subsurface environment. Continuous exposure to nitrate contamination can be dangerous for humans, leading to several types of cancer (De Roos et al. 2003; Ward et al. 2005) and an increase of methemoglobin in the blood (Johnson et al. 1987). For several decades, the increase of nitrate concentrations in groundwaters has caused degradation of water quality all over the world, and especially in karst environments (Nolan and Stone, 2000; Li et al. 2010; El Gaouzi et al. 2013; Schwientek et al. 2013; Alexia et al. 2015; Musgrove et al. 2016; Opsahl et al. 2017; Bu et al. 2017; Briand et al. 2017; Yue et al. 2019; Yang et al. 2019; Wang et al. 2020). Nitrate load export at the output of karst system can be high (Eller et al. 2017) and can imply a degradation of water quality in the receiving environment.

The origin of nitrate nitrogen needs to be identified in order to identify water resource hazards due to nitrate contents, either through direct inputs (atmospheric deposition, fertilizer) or through the transformation of nitrogen applied and transformed from the unsaturated zone to the groundwaters. Hence, knowledge about origins of the nitrate contamination is the first step for implementation of remediation measures to protect the water resources and avoid further water quality deterioration. In a complex hydrogeological context, the measurement of nitrate concentrations alone does not allow to determine their origin. On the other hand, the combined approach of hydrochemistry and isotope biogeochemistry could be a very relevant tool to better determine the origin of nitrogen in a particularly difficult context, with complex hydrogeological relationships between several karst aquifers both confined and unconfined. For several years, natural abundance stable isotope measurements of nitrate ($\delta^{15}N$ and $\delta^{18}O$) have been used to identify its origins, including karst environment (Panno et al. 2001; Liu et al. 2006; Briand et al. 2017; Valiente et al. 2020). Typically, as a function of the pedo-climatic context and linked with land-use, nitrate can arise from: (i) primary sources such as atmospheric nitrate (Panno et al., 2001) or synthetic nitrate fertilizer; (ii) secondary sources such as synthetic ammonium fertilizer (Panno et al. 2001; Liu et al. 2006; El Gaouzi et al. 2013), sewage (Liu et al. 2006; Li et al. 2010; El Gaouzi et al. 2013; Briand et al. 2017; Yang et al. 2019), or manure (Li et al. 2010; Heaton et al. 2012) with potential volatilization and subsequent nitrification. Due to the extent of these processes and the associated isotopic fractionation, the range of $\delta^{15}N$ and $\delta^{18}O$ values of nitrate can vary significantly especially for ^{15}N (Kendall et al. 2007).

These nitrate sources have distinct isotopic signatures, which can be used to semi-quantify the relative contribution of a single nitrogen (N) source (Aravena et al. 1993; Yakolev et al. 2015; Grimmeisen et al. 2017). In the case of a secondary source of N, where nitrate is produced after transformation in the soil that modify its concentration, fractionate

its isotopes and which can blur the initial signature of the N sources (Böttcher et al. 1990; Kendall et al. 2007; Briand et al. 2017). Besides their widespread use for determining the origins of nitrate, $\delta^{15}N_{-NO3^-}$ and $\delta^{18}O_{-NO3^-}$ can also be extended as a tool to characterize the way of functioning of multilayered karst aquifers and can be used as tool for better water management.

The proposed approach is applied to the Toulon multilayered karst system, located in the Southwest of France. It is a good example of a multilayered karst aquifer, with an outlet fed by two multilayered karst aquifers (Lastennet et al. 2004; Lorette et al. 2017, 2018, 2020). For more than 60 years, increasing nitrate concentrations at the outlet of Toulon karst system have justified the implementation of the isotopic approach all over the hydrogeological catchment. This is a foremost concern as it serves as a major source of drinking water for approximately 55 000 people.

The objective of this paper is to use an isotopic approach to evaluate nitrate vulnerability in karst aquifers in order to sustainably manage the water resource.

Specifically, this research would like to: (i) assess nitrate sources in the Toulon Springs hydrogeological catchment; (ii) identify relationships between confined and unconfined karst aquifers using nitrate isotopes proposing a conceptual framework of the hydrogeochemical functioning of the Toulon multilayered karst system associated with nitrogen transport ; and (iii) from a more fundamental standpoint, provide a set of parameters adapted for karstic hydrogeological catchment and lays the foundation for the use of isotope biogeochemistry as a powerful tool for understanding the recharge of drinking water catchments and beyond the efficient management of water quality at the scale of karstic hydrogeological catchment.

2. Site description

2.1 Geology and hydrogeology

The Toulon Springs have supplied drinking water to the city of Périgueux (France) since 1832. It is a Vauclusian-type spring, located on a major faulted anticlinal structure, oriented N145° (Lastennet et al. 2004). The Toulon Springs are the main perennial outlet of the Toulon karst system and can reach almost 1 000 $L.s^{-1}$ during rainfall events, with a mean annual daily discharge of 450 $L\ s^{-1}$ (Lorette et al. 2018; Lorette, 2019).

The geology of the area is composed of carbonated rocks from upper Cretaceous and middle-upper Jurassic carbonate rocks (Fig. 1), the Cretaceous rocks are 200-250 meters in thickness(Turonian, Coniacian, Santonian, Campanian) and the Jurassic rocks 300-350 meters in thickness (Bajocian, Bathonian, Oxfordian, Kimmeridgian) (Von Stempel, 1972; Lorette, 2019). The Cretaceous rocks at the top are limestones, while the Jurassic rocks below are dolomitic limestone and dolomites. There is an epikarst above the carbonate rocks topped by a soil layer of few meters. The Toulon karst system also presents a fold and faults mainly oriented NW-SE (Fig. 1).

The hydrogeological situation comprises three main multilayered aquifers: (i) an unconfined karstic upper Cretaceous aquifer: Turonian, Coniacian and Santonian aquifers, (ii) a confined karstic upper Jurassic aquifer: Oxfordian and Kimmeridgian aquifer and (iii) a confined karstic middle Jurassic aquifer: Bajocian and Bathonian aquifer. Cenomanian marls, considered impermeable, separate the upper Cretaceous aquifer and the upper Jurassic aquifer. The upper Cretaceous aquifer and the upper Jurassic aquifer are separated by Cenomanian marls, considered impermeable, Spatial thickness (4-20 meters) and facies

158 variations (marls-sand) over the study area entail additional difficulties in understanding the
159 relationship of the two main aquifers.

160 The Toulon Springs hydrogeological catchment is composed of three main rivers: (i)
161 the Isle River, consider as the regional base level; (ii) the Beauronne River in the northern
162 part of the study area; (iii) the Foncroze River, in the southern part of the aquifer.

163 The hydrogeological dynamic of the Toulon Springs has been explained by Lastennet
164 et al. (2004) and Lorette et al. (2017, 2018, 2020). The system is an example of springs
165 originating from a confined Jurassic aquifer and an unconfined Cretaceous aquifer according
166 to the hydrogeological conditions. During the low-flow period, there is a large water input
167 from the confined Jurassic aquifer and the saturated part of the unconfined Cretaceous
168 aquifer (Turonian). This implies that the Jurassic aquifer has a reservoir function. In a high-
169 water period, infiltration water activates the drainage network in the formations above the
170 Turonian (*i.e.* Coniacian and Santonian), thus suggesting that the Cretaceous aquifer has a
171 transmission function. The Cretaceous aquifer is responsible for the hydrodynamic and
172 hydrochemical variations. This enables the rapid transmission of the contaminants from the
173 surface and subsurface. In terms of surface infiltration (*e.g.* NO_3^-, DOC, bacteria, and
174 turbidity), the Cretaceous aquifer contributes to the water quality hazards of the Toulon
175 springs (Lorette et al. 2020).
176

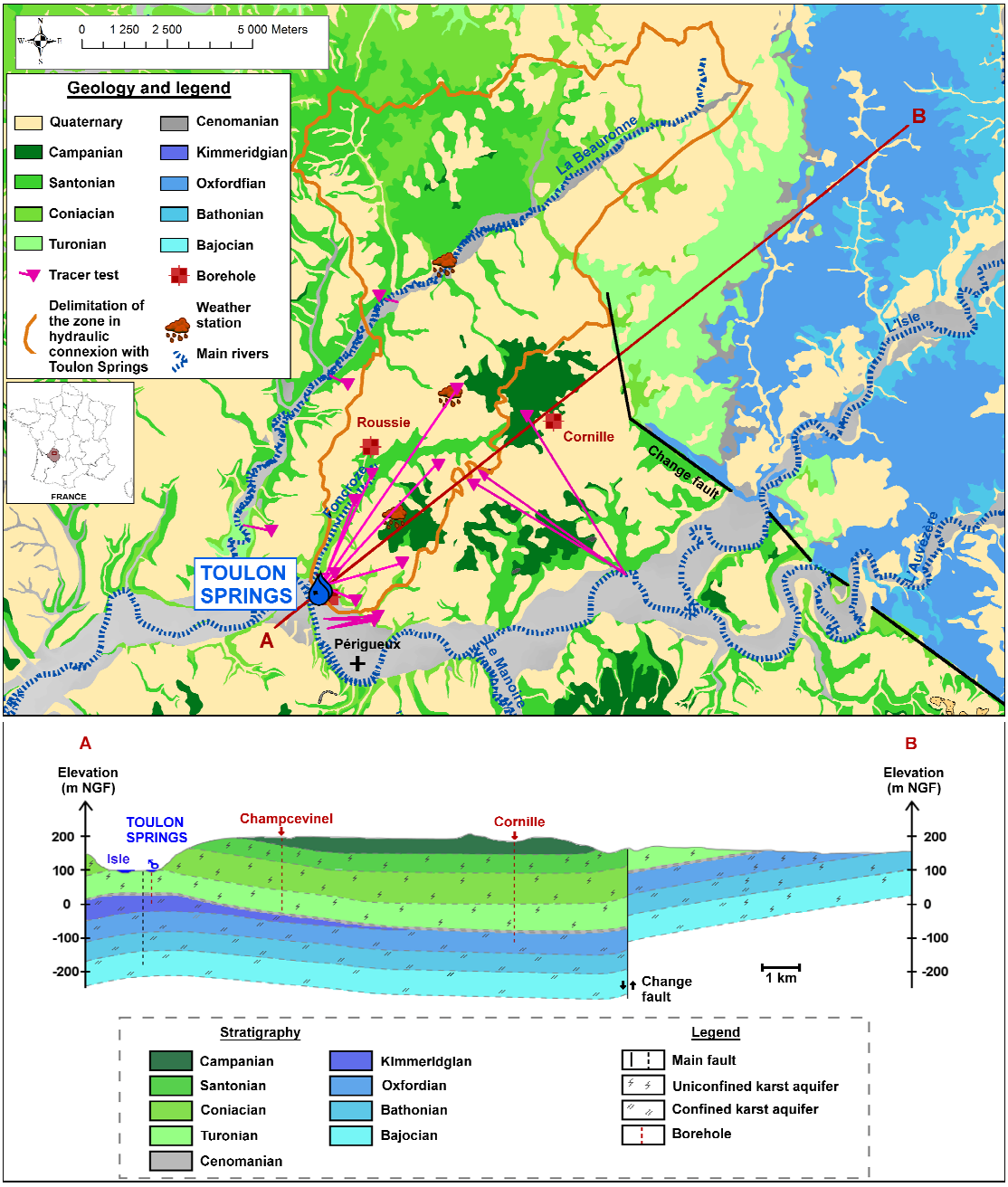

Fig. 1 : Hydrogeological map of the Toulon multilayered karst aquifer. AB: simplified SW-NE geological cross-section. The Cenomanian is considered as non aquifer (adapted from Lorette et al. 2018).

184 ## 2.2 Land use and nitrate loads

185

186 Typical karstic landforms can be found on the area's land surface. There are several
187 exokarstic forms such as sinkholes and surface water loss (*e.g.* stream river loss) on the
188 plateau above the Toulon springs. Most of the losses are temporary and activated only after
189 heavy rains. Sinkholes are mostly located on the plateau, in the thin soil layer area. In karst
190 environments, a tracer test is an effective tool to understand the relationships between karst
191 landforms and the outlet karst systems (Atkinson et al. 1973; Geyer et al. 2007; Labat and
192 Mangin, 2015; Mudarra et al. 2014; Marin et al. 2015; Sivelle and Labat, 2019). Over the
193 study area, tracer tests (Fig. 1) show flow between 6.4 m h^{-1} and 130 m h^{-1}, testifying to the
194 karst vulnerability of the hydrosystem.

195 The dominant land uses of the rural area in the northern part of the city of Périgueux
196 are forestry (47 %) and agricultural (43 %). Urban areas represent only 10 % of the
197 catchment surface (Lorette, 2019). Agricultural areas are dominated by crops of wheat, corn,
198 sunflower, and colza. Nitrogen is applied as ammonium nitrate (NH_4NO_3 - N synthetic
199 fertilizer) and sewage sludge. Although accounting for only 10 % of land use, the influence
200 of dwellings on nitrogen support is also noteworthy. On the whole study area, ~1 500 houses
201 have septic tank, causing concentrated nitrogen inputs. Since the 1960's, the increase of
202 intensive agriculture with the increase of nitrogen inputs has been responsible for the
203 significant increase of nitrate concentrations in the Toulon springs (Fig. 2A).

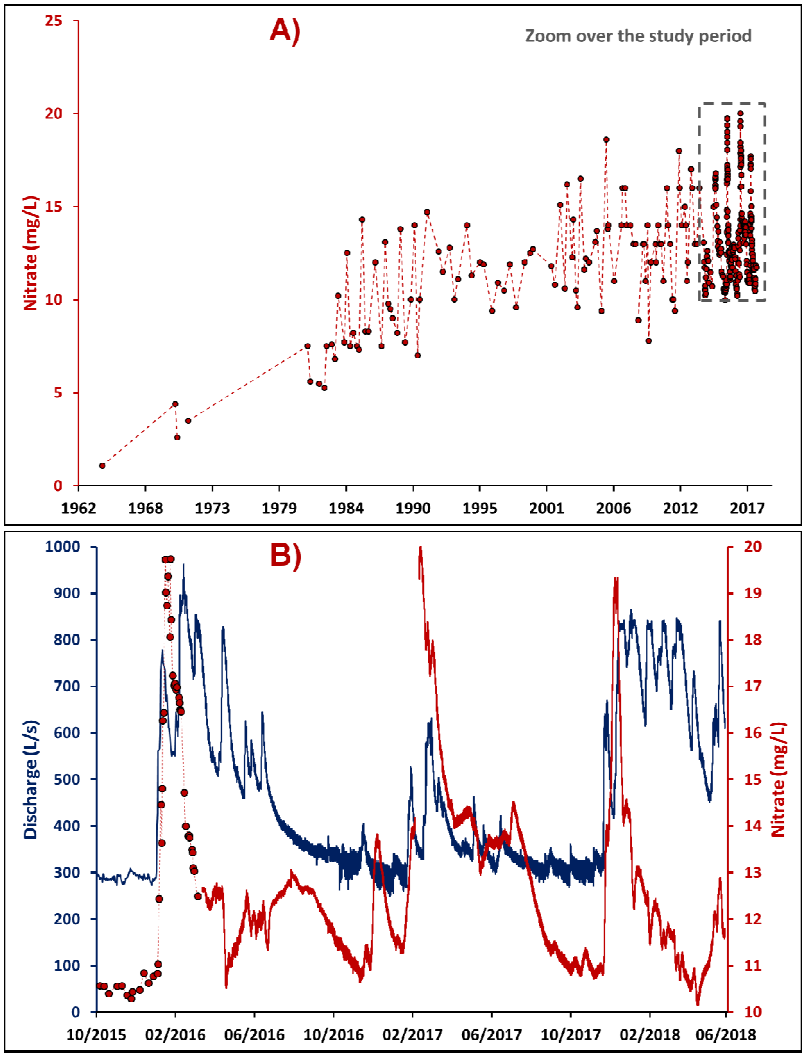

204

205 **Fig. 2 : A) Temporal evolution of nitrate concentration at the Toulon Springs from 1962 to 2018. B) Temporal**
206 **evolution of discharge and nitrate concentration at the Toulon Springs from 01/10/2015 to 20/06/2018 (adapted from**
207 **Lorette et al. 2018 and Lorette, 2019).**
208

209 The local hydrochemical background was ~1 mg L^{-1} in 1962 at low-flow conditions
210 and is now close to ~12 mg L^{-1} on average with a maximum peak concentration of
211 ~20 mg L^{-1} during floods (Fig. 2B). In addition to data provided by administration of
212 Dordogne from 1960 to 2016, higher frequency measurements have been taken since 2016
213 (Lorette, 2019). Previous studies conducted in the Toulon Springs have demonstrated a
214 yearly export of 40 TN (Lorette, 2019). Nitrate stored in the unsaturated zone of the aquifer
215 may be transported to the saturated zone after some rainfall events (Lorette et al. 2020). At
216 the outlet of the karst system, nitrogen discharge as nitrate from the Toulon springs, come

from continuous inputs over the hydrogeological catchment. The resulting dynamic of changing nitrate concentration over time depends on its storage, transformation, and transfer from the soil-unsaturated zone to the outlet.

3. Material and methods

3.1 Sampling strategy

The main sampling strategy aimed to evaluate the water quality in both surface waters and groundwaters, with a focus on nitrate contamination. Sampling stations were selected to be representative of each karst aquifer in both confined and unconfined parts, as a function of knowledge of the study area and previous field investigations. To do so, hydrogeochemical and isotope measurements were done in order to characterize nitrate end-members and fate in the Toulon multilayered karst system.

From October 2015 to November 2017, hydrogeochemical data (physico-chemical parameters, major ion concentrations, nutrient concentrations) and isotopic data ($\delta^{15}N_{-NO3^-}$, $\delta^{18}O_{-NO3^-}$) were measured in springs, boreholes, and rivers over the Toulon multilayered karst system. In addition, $\delta^{15}N$ and $\delta^{18}O$ of nitrate were measured on an ad hoc basis on potential nitrate sources over the study area.

3.1.1 Collection of groundwaters and surface waters

At the Toulon Springs, water samples were collected twice a month from October 2015 to January 2017, with daily sampling during groundwater flood events. A total of 51 samples

241 were collected. High resolution analyses of nitrate concentration have also been conducted
242 since March 2016 using an UV-visible scanning spectrophotometer (Spectro::lyser, S::CAN),
243 with a precision of 0.1 mg L^{-1}, and a 0 to 46 mg L^{-1} range of measurement. To avoid
244 measurement errors due to matrix interference when turbidity increases, a manual calibration
245 of the Spectro::lyser was done with laboratory measurements (Lorette, 2019).

246 Three sampling campains were conducted under different hydrological conditions:
247 November 2015 (T1), representative of the water quality during low flow conditions; January
248 2016 (T2), representative of water quality during the first flood of the hydrological cycle;
249 May 2016 (T3), representative of the water quality during a spring flood. Each campain was
250 conducted at least 3 days after rainfall event, to avoid direct contribution of atmospheric
251 nitrate from rainfall to both surface water and groundwater.

252 17 springs, 4 boreholes, and 7 samples in rivers were sampled during the T1, T2, and
253 T3 campains. A total of 65 samples were collected over the whole study area during sampling
254 campains, 13 from rivers, 45 from springs, 7 from boreholes.

255 Water samples were filtered in the field using a 0.45 µm PVDF membrane and divided
256 between three bottles: (i) 50 mL polyethylene bottle for anion concentration measurement,
257 (ii) 50 mL polyethylene bottle and acidified in the field to pH = 2 with HNO_3 for cation
258 concentration measurement, and (iii) 150 mL was also filtered in the field on a 0.20 µm
259 PVDF membrane, poisoned with $HgCl_2$ (6%), and dispatched into polyethylene bottle for the
260 measurement of $\delta^{15}N$ and $\delta^{18}O$ values of nitrate.

261 The groundwater samples were mainly collected in the upper Cretaceous karst aquifer
262 (96 samples - GW1 to GW15; B2). The other samples were collected in Jurassic karst aquifer
263 (7 samples - GW16 and GW17; B4). B1 and B3 capture both Turonian aquifer and upper
264 Jurassic aquifer (Oxfordian, Kimmeridgian).

265

3.1.2 Sewage, fertilizer, soils, and rainwater.

In order to better constrain the isotopic range of nitrogen sources, sampling was carried out before the water reaches the soil, the unsaturated zone and the aquifer.

Rainwater samples (NS1) were collected in the rain gauge (Fig. 3), 3 km north of the Toulon Springs. Sewage samples (NS2) were collected before discharge into the Beauronne River (Fig. 3). Solid samples of ammonium nitrate (NS3), representative of synthetic N fertilizer used over the hydrogeological catchment, were provided by local farmers, assuming that all the farmers use the same type of fertilizer and buy from the same supplier.

In addition to the characterization of primary sources of N, soil samples were collected in order to integrate variations in primary sources of N in the soil according to different types of inputs. An agricultural soil (NS4), representative of soil where N synthetic fertilizers are amended, was sampled (Fig. 3). Finally, agricultural soils (NS5), which have received amendments in the form of sewage sludge applications were sampled (Fig. 3).

The same collection bottles were used for liquid samples (NS1, NS2) as for groundwater and river water samples.

For soils samples (NS4, NS5), extraction of nitrate was performed with 0.5 M KCl to determine the isotopic composition of nitrate in the soil. Details are given in Briand et al. (2017).

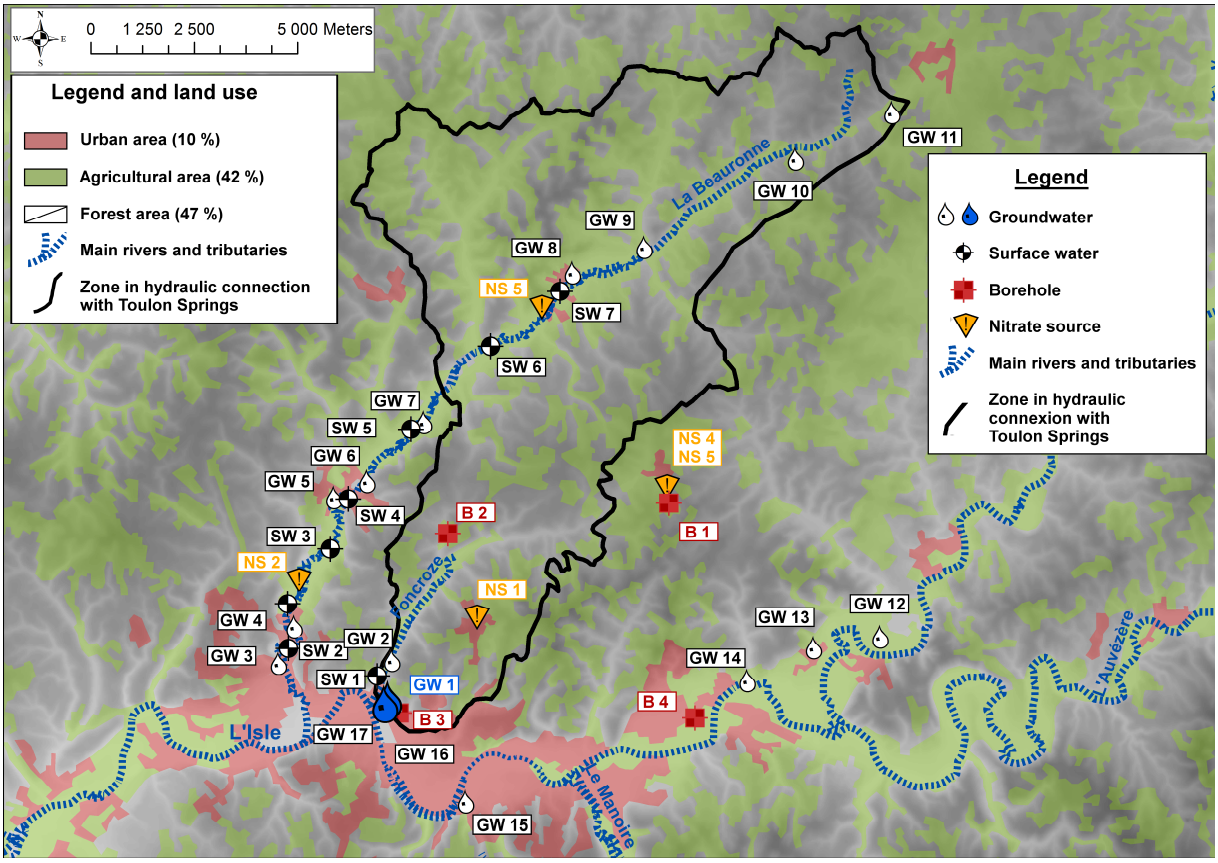

Fig. 3 : Land use and sampling position over the Toulon hydrogeological catchment.

3.2 Analytical methods

In the field, a multiparameter WTW 3430 was used for temperature (T), pH (pH), electrical conductivity (EC) and dissolved oxygen concentration measurements (O_2), precise to ±0.1°C, ±0.05, ±1µS cm^{-1}, and ±0.1 mg L^{-1} respectively. Alkalinity was measured within 12 hours, by acid titration at the laboratory I2M-GCE in Bordeaux.

Ion concentrations (Ca^{2+}, Mg^{2+}, Na^{+}, K^{+}, Cl^{-}, NO_3^{-} and SO_4^{2-}) were determined by chromatography using a Dionex ICS 1500 for the cations and using a Dionex ICS 1100 equipped (measurement accuracy 2%).

$\delta^{15}N$ and $\delta^{18}O$ values of NO_3^{-} were determined using the azide method modified from McIlvin and Altabet (2005) with a purge and trap IRMS system (DeltaVplus, Thermo

Scientific, Bremen, Germany) in continuous-flow with a purge and trap system coupled with a Finnigan GasBench II system (Thermo Scientific). Details are given in Semaoune et al. 2012, Briand et al. 2017, and Sebilo et al. 2019. Results are reported in the internationally accepted delta notation in ‰ with respect to the standards air for $\delta^{15}N$ and Vienna Standard Mean Ocean Water (V-SMOW) for $\delta^{18}O$, respectively. Nitrate and nitrite reference materials subject to the same analytical procedures were used to calibrate the isotopic composition of N_2O (USGS34, $\delta^{15}N$ = -1.8 ‰, $\delta^{18}O$ = -27.9 ‰, USGS35, $\delta^{15}N$ = +2.7 ‰, $\delta^{18}O$ = +57.5 ‰ and USGS32, $\delta^{15}N$ = +180 ‰, $\delta^{18}O$ = +25.7 ‰ for nitrate standards; lab nitrite standards Lb1, $\delta^{15}N$ = -63‰ and Lb2, $\delta^{15}N$ = +2.7 ‰ for nitrite standards). The precision was ± 0.3 ‰ for $\delta^{15}N$ values and ± 0.5 ‰ for $\delta^{18}O$ values of nitrite.

For solid samples of fertilizer (NS3), samples were air-dried, ground, and sieved through a 1 mm mesh. Total nitrogen contents were determined using an elemental analyzer (Elementar). Isotope abundance ratios of total nitrogen for soils were determined by continuous-flow isotope ratio mass spectrometry coupled with an elemental analyzer (EA-CF-IRMS). Cup samples were then analysed N elemental and isotopic compositions using an elemental analyser (EA; NC2500, CarloErba®) coupled with an isotope ratio mass spectrometer (IRMS; Isoprime, GV Instruments®). IRMS daily drift was monitored using homemade standards (caseine, glycine) and, if necessary, data were corrected consequently. Elemental composition was calibrated against acetanilide and isotopic composition against homemade standards and reference material (IAEA-N_2).

3.3 Hydrological approach

The origin of the nitrate present in the Toulon Springs could be inorganic and/or organic and direct or indirect. Inorganic nitrate is the nitrate itself contained in rainfall and

inorganic fertilizers. It can also be nitrate produced from the nitrification of ammonitrate in the soil. Organic nitrate arises from the production of nitrate from the ammonification and nitrification of organic matter and then its nitrification (Sebilo et al. 2013).

The isotopic composition of nitrate in the Toulon Springs, as the main outlet of the karst system, could be an integration of the isotopic signatures of nitrate for different nitrogen pools within the hydrogeological catchment. According to the large $\delta^{15}N$ and $\delta^{18}O$ values of NO_3^- range of potential sources measured in literature (Kendall et al. 2007), it was necessary to: (i) confirm that the data obtained were in agreement with those presented in the Kendall plot; and (ii) better define these range of values for the studied area to precisely identify the isotopic signatures of nitrate sources. These range of potential sources are usually represented by rectangles in $\delta^{15}N_{vs}\delta^{18}O$ diagram (Panno et al. 2001; Kendall et al. 2007; Heaton et al. 2012; Briand et al. 2017), theoretically integrating the set of possible isotopic signatures. In this work, the redefinition of range of values aimed to reduce the rectangle size in the $\delta^{15}N_{vs}\delta^{18}O$ diagram.

The data of potential sources were plotted with data from surface waters, groundwaters and the Toulon Springs in the $\delta^{15}N_{vs}\delta^{18}O$ diagram. At each corner of the rectangles, arrows of 0.5 slope are drawn, representing the denitrification process. It is considered that any point which lies between the two arrows from the same potential source (or rectangle) will have the potential source as an initial isotopic signature and will undergo a denitrification process causing a deviation from the initial signature.

Once relationships are established between the parameters, the data is integrated in the hydrogeological context for a better explanation of the way karst system functions and to help the water management over the hydrogeological catchment.

3.4 $\delta^{15}N_{-NO_3^-}$ and $\delta^{18}O_{-NO_3^-}$ of potential sources.

In a karstic context of the study, it is thus even more important to take into account the direct sources of nitrogen, likely to be able to infiltrate directly into the groundwater, and the indirect sources, likely to confer an isotopic signature of the nitrate that does not reflect the mixture of the direct sources (Fig. 4). The direct inputs of nitrate nitrogen on the catchment should be a mixture of atmospheric deposition and inorganic fertilizers (Fig. 4).

The basic idea behind the use of isotope biogeochemistry is that the measurement of the isotopic composition of nitrate at a definite location and time within a catchment reflects: (i) the endmembers, direct sources from which it originates, and (ii) the processes responsible for variations in its concentration.

$\delta^{15}N$ and $\delta^{18}O$ values of nitrate in the unsaturated zone (USZ) integrate on the one hand the isotopic composition of the potential direct sources of nitrogen (atmospheric deposition, inorganic fertilizers), and on the other hand the isotopic composition of nitrate resulting from biogeochemical processes in the soil which represent indirect source of nitrate nitrogen.

The ammonification and nitrification of nitrogen contained in organic matter (soils, manure, slurry) leads to the production of nitrate whose isotopic composition does not reflect the exogenous nitrogen inputs (atmospheric deposition and inorganic fertilizers), but their assimilation, production and re-production of nitrate from the dynamic of soil organic matter (El Gaouzi et al. 2013; Sebilo et al. 2013; Briand et al. 2017). Moreover, volatilization of NH_4^+, non-complete nitrification and denitrification in the USZ could induce a significant isotopic fractioning which could impact the isotopic composition of the nitrate pool leaving the unsaturated zone and reaching the saturated zone. Finally, nitrate could be a product of the biological transformation of sewage, sludge spreading and more generally the ammonification-nitrification of organic matter within the soils (Fig. 4).

It has been established that nitrate diffusion and advection do not generate a significant isotopic fractioning (Semaoune et al. 2012). Thus, provided that no biogeochemical processes take place during the infiltration of nitrate into groundwater, the isotopic composition of nitrate reaching the groundwater table should reflect that of nitrate leaving the biogeochemically reactive unsaturated zone.

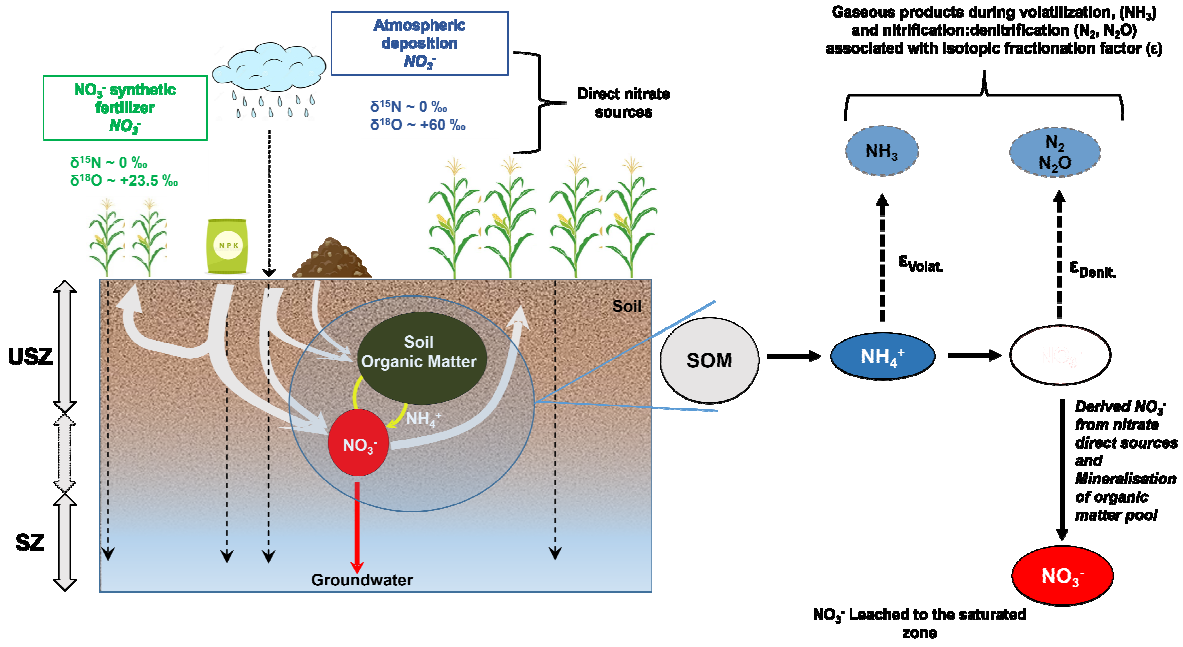

Fig. 4 : Schematic N transformation from direct nitrate sources in the N cycle associated with isotopic transformation in the unsaturated zone (USZ) and transfer to the saturated zone (SZ).

4. Results and discussion

Tables presenting the data in the following sections are proposed in the supplementary data.

4.1 Hydrochemical background and nitrate concentration in groundwater

Upper Jurassic karst aquifers have a typical deep water signature, with warm water (between 17.3 °C and 20.6 °C), and low dissolved oxygen concentrations (between 3.3 mg L^-

[1] and 0.1 mg L^{-1}). Dolomitic limestone and long residence time imply high magnesium concentrations in upper Jurassic karst aquifers (between 21.1 mg L^{-1} and 23.2 mg L^{-1}) (Fig. 5A).

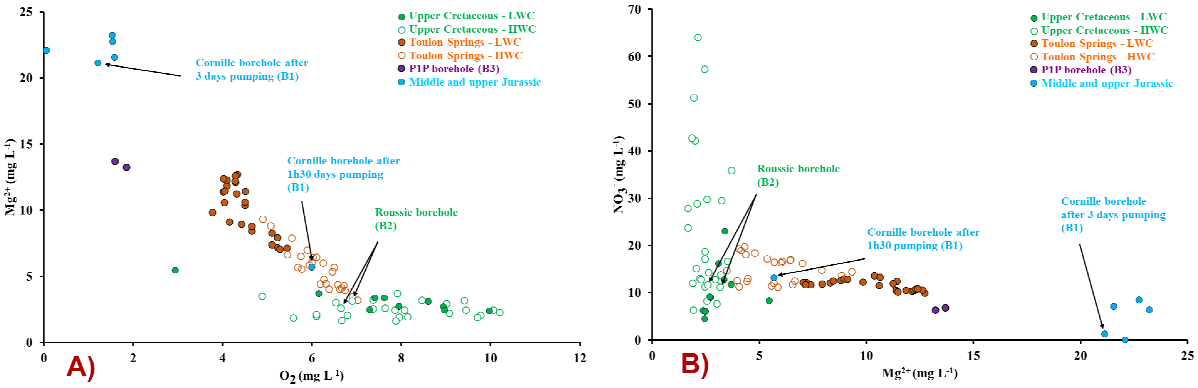

Fig. 5 : A) $O_{2vs}Mg^{2+}$ binary plot performed with groundwater over the Toulon Springs hydrogeological catchment. B) $Mg^{2+}{}_{vs}NO_3^-$ binary plot performed with groundwater over the Toulon Springs hydrogeological catchment.

The anoxic condition of these aquifers suggests a confined character, which is not typical in karstic environments (Mahler and Bourgeais, 2013; Lorette et al. 2018). Water from the Cornille borehole (B1) is a mix between Turonian aquifer and upper Jurassic aquifer (Oxfordian, Kimmeridgian). The two samples at the the Cornille borehole were not collected under the same conditions. 05/11/2015 sample was performed after 1h30 pumping and 18/09/2017 after 3 days of pumping, with a same pumping discharge of 100 m^3 h^{-1}. Water geochemical facies is characteristic of a mix between the two aquifers, with dissolved oxygen concentration, magnesium concentration, and nitrate concentration respectively of 2.3 mg L^{-1}, 5.7 mg L^{-1} and 13.1 mg L^{-1} (Fig. 5B). 18/09/2017 sample was performed after three days pumping. Water geochemical facies is characteristic of upper Jurassic aquifer, with dissolved oxygen concentration, magnesium concentration, and nitrate concentration respectively of 1.2 mg L^{-1}, 21.1 mg L^{-1} and 1.3 mg L^{-1}. The Trelissac borehole (B4) captures middle Jurassic aquifer (Bajocian, Bathonian). Water hydrogeochemical facies is characteristic of this deep

413 aquifer, with very low dissolved oxygen concentration (0.1 mg L^{-1}), and high magnesium
414 concentration (22.1 mg L^{-1}) (Fig. 5A). No nitrate concentration is recorded in the middle
415 Jurassic aquifer. ^{14}C dating have shown a relative age of 12 500 years from middle Jurassic
416 aquifer (unpublished data).

417 Upper Cretaceous karst aquifers (Turonian, Coniacian, Santonian) are characterized
418 with a calcium bicarbonate facies. Magnesium concentrations are lower in Cretaceous
419 aquifers than in Jurassic aquifers, as a result of the absence of dolomite (between 1.7 mg L^{-1}
420 and 5.5 mg L^{-1}). As usual in karst environments, water could be considered oxic with
421 O_2 > 6 mg L^{-1}. (Perrin et al. 2007; Mahler et al. 2011; Musgrove et al. 2011). The Roussie
422 borehole (B2) is a typical borehole capturing upper Cretaceous aquifer (Turonian,
423 Coniacian), with a low magnesium concentration compared to Jurassic aquifers (3.1 mg L^{-1}
424 and 2.6 mg L^{-1}). Nitrate concentrations are similar both for the two samples (11.2 mg L^{-1} and
425 11.7 mg L^{-1}) (Fig. 5B). Dissolved oxygen concentrations highlight oxic water, with similar
426 concentrations both for the two samples (6.9 mg L^{-1} and 6.7 mg L^{-1}). The P1P borehole (B3)
427 is representative of the Turonian saturated zone near Toulon Springs. Next to the outlet of the
428 karst system, upper Jurassic aquifer mixes with Turonian aquifer (Lorette et al. 2018). Mean
429 dissolved oxygen concentration, mean magnesium concentration, and mean nitrate
430 concentration are respectively 1.7 mg L^{-1}, 13.5 mg L^{-1}, and 6.6 mg L^{-1} (Fig. 5B). The Toulon
431 Springs water hydrogeochemical facies is close to the P1P borehole according to its
432 hydrogeological characteristics. Dissolved oxygen concentration (minimum value of 3.8 mg
433 L^{-1}) is consistent with the higher participation of the upper part of the upper Cretaceous
434 aquifer (Lorette et al. 2018).
435
436 During low water conditions, the surface water (Beauronne River, Foncroze River) has
437 minimum and maximum nitrate concentrations of 5.8 and 6.2 mg L^{-1}.

438 During flood events, mean nitrate concentrations have been found to be higher than
439 during low water conditions, with mean nitrate concentrations of 25.4 mg L^{-1} and 18.1 mg L^{-1}
440 respectively, for both January 2016 and May 2016 floods.
441 The mean nitrate concentration for groundwater is higher than in surface water. During
442 2015 low flow conditions, the mean groundwater nitrate concentration was 17.5 mg L^{-1}, with
443 minimum and maximum values of 8.5 mg L^{-1} and 47.4 mg L^{-1} respectively (Fig. 5B). During
444 January 2016 flood, nitrate concentrations increased in most springs, with a mean
445 concentration of 25.9 mg L^{-1}, with a minimum and maximum values of 6.4 mg L^{-1} and
446 64.1 mg L^{-1} respectively (Fig. 5B).
447 The Toulon Springs samples which were taken over more than one hydrological cycle
448 (06/10/2015 to 04/01/2017) allowed us to analyse nitrate concentrations during several flow
449 conditions (flood, recession, depletion). The mean nitrate concentration value was 13.4 mg L^{-1},
450 with minimum and maximum concentrations of 10.0 mg L^{-1} on 25/11/2015 and 19.8 mg L^{-1}
451 on 18/01/2016 respectively. High resolution monitoring highlights the evolution of nitrate
452 concentrations at the outlet of the karst system. During flood events, the increase or decrease
453 in nitrate concentrations recorded at the Toulon Springs, imply no linear relationships
454 between nitrate and discharge. Increase or decrease in nitrate concentrations have already
455 been recorded in previous studies and are associated with leaching of the soil and unsaturated
456 zone of the aquifer (Rowden et al. 2001; Stueber and Criss 2005; Mahler et al. 2008; Pronk et
457 al. 2009; Pu et al. 2011; Huebsch et al. 2014). During low water conditions, nitrate
458 concentrations decreased, this is linked with the increased participation of the deep upper
459 Jurassic aquifer. The earliest analyses of the Toulon Springs suggest nitrate levels were very
460 low in the 1960's, but rose substantially by the 1970s (Fig. 2). Today the mean concentration
461 is about 12 mg L^{-1} but can reach more than 20 mg L^{-1} during some flood events.
462

463 **4.2 Isotope data**

464

465 $\delta^{15}N$ and $\delta^{18}O$ values of nitrate in surface waters, in groundwaters and in potential
466 sources are summarized in tables of the supplementary data.

467 $\delta^{15}N_{-NO3^-}$ and $\delta^{18}O_{-NO3^-}$ values for rainwater is -5.4 ‰ and +61.3 ‰ respectively.

468 $\delta^{15}N$ values for synthetic inorganic fertilizers used over the hydrogeological catchment
469 of the Toulon Springs are +0.9 ‰ and +1.1 ‰, and are within the typical ranges reported for
470 fertilizers in other countries (Vitoria et al. 2004; Bateman and Kelly, 2007; Heaton et al.
471 2012; Briand et al. 2017).

472 $\delta^{15}N_{-NO3^-}$ and $\delta^{18}O_{-NO3^-}$ values for cultivated soil are respectively between -1.9 ‰ and
473 +1.3 ‰ for $\delta^{15}N_{-NO3^-}$, and between +0.2 ‰ and +2.2 ‰ for $\delta^{18}O_{-NO3^-}$ (Fig. 6).

474 $\delta^{15}N_{-NO3^-}$ and $\delta^{18}O_{-NO3^-}$ values for soil where sewage sludge were applied, are
475 respectively between +10.9 ‰ and +33.8 ‰ for $\delta^{15}N_{-NO3^-}$, and between +27.0 ‰ and
476 +57.5 ‰ for $\delta^{18}O_{-NO3^-}$ (Fig. 6).

477 $\delta^{15}N_{-NO3^-}$ and $\delta^{18}O_{-NO3^-}$ values for sewage are respectively between -1.9 ‰ and +6.3 ‰
478 for $\delta^{15}N_{-NO3^-}$, and between -4.2 ‰ and -2.9 ‰ for $\delta^{18}O_{-NO3^-}$ (Fig. 6).

479 Isotopic signatures from potential sources measured over the hydrogeological
480 catchment are consistent with the data found in literature but ranges of values (or rectangles)
481 in Fig. 6 are reduced, illustrating the need for precision in ranges of values. In other words,
482 the data obtained are in good agreement with those presented in the "Kendall plot" and better
483 define these ranges of values for the hydrogeological catchment, and are used to accurately
484 identify the isotopic signatures of nitrate sources. An illustration of our potential sources in a
485 Kendall plot is given in supplementary information.

486

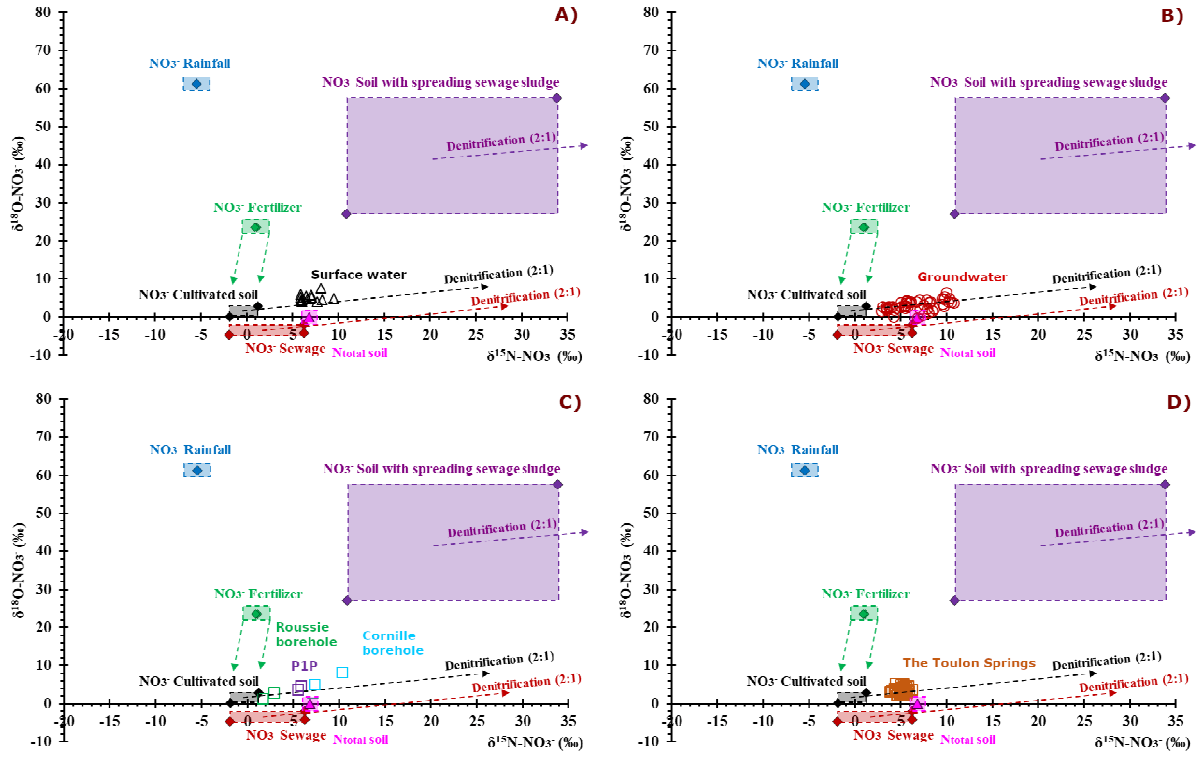

Fig. 6 : $\delta^{15}N_{-NO_3^-}$ and $\delta^{18}O_{-NO_3^-}$ measured in nitrate potential sources, surface water (A), groudnwater (B), boreholes (C), and the Toulon Springs (D).

$\delta^{15}N$ and $\delta^{18}O$ values of nitrate in surface water (SW1 to SW7) and in groundwaters (GW1 to GW17) are from +3.4 ‰ to +10.8 ‰ for $\delta^{15}N_{-NO_3^-}$, and from -0.1 ‰ to +7.6 ‰ for $\delta^{18}O_{-NO_3^-}$ (Fig. 6).

For boreholes, $\delta^{15}N$ and $\delta^{18}O$ values of nitrate vary between +1.7 ‰ and +10.3 ‰ for $\delta^{15}N$ and between +1.3 ‰ and +9.3 ‰ for $\delta^{18}O$ (Fig. 6). The most depleted and enriched were measured respectively for the Roussie borehole (upper Cretaceous aquifer) and in the Cornille borehole (mix between upper Jurassic and upper Cretaceous aquifers).

Concerning the Toulon Springs, the isotope compositions of nitrate are between +3.8 ‰ and +6.2 ‰ for $\delta^{15}N_{-NO_3^-}$ and between +2.2 ‰ and +5.4 ‰ for $\delta^{18}O_{-NO_3^-}$ (Fig. 6). No linear relationship between $\delta^{15}N_{-NO_3^-}$ and discharge (or water condition) is highlighted.

Isotopic signatures measured in the area environment (surface water, groundwater, boreholes, and the Toulon Springs) are not located in rectangles. Data are well distributed along the 2:1 (Fig. 6) expected residual nitrate derived from denitrification (Böttcher et al. 1990; Kendall et al. 2007; Singleton et al. 2007; Liu et al. 2013).

4.2.1 Input of nitrate direct sources

Rainfall is the main source for aquifer recharge. NO_3^- concentrations from rainfall were measured at 1.4 mg L^{-1} on 23/05/2016 with an average concentration of 1.4 mg L^{-1} between October 2015 and October 2018 (Lorette, 2019).

Over the study area, the isotopic compositions of rainfall were measured at -5.4 ‰ for $\delta^{15}N_{-NO3^-}$ and +61.3 ‰ for $\delta^{18}O_{-NO3^-}$, which are close to values measured in other regions across the world (Panno et al. 2001; Yue et al. 2017; Li et al. 2019). Despite the low nitrate concentrations, rainfall contributes about 49 tones per year of nitrogen (TN $year^{-1}$) over the Toulon Springs hydrogeological catchment (Lorette, 2019). However, this nitrogen source is very attenuated by biogeochemical processes occurring in the soil. Previous studies (Katz et al. 2009; Lombardo Associates, 2011; El Gaouzi et al. 2013; Briand et al. 2017) have shown the isotopic signature of rainfall is totally lost when nitrate reaches the soil because it is assimilated into soil organic matter. Hence, only occasional infiltration events from sinkholes can highlight this isotopic composition at the outlet of a karst system (Panno et al. 2001).

N synthetic fertilizers (ammonium nitrate) have been applied for years over the catchment. Ammonitrate were produced following the Haber-Bosch process using nitrogen and oxygen of the air with $\delta^{15}N_{-N2}$ = 0 ‰ and $\delta^{18}O_{-O2}$ = +23.5 ‰). N synthetic fertilizer have

526 a $\delta^{15}N_{-NO3^-}$ close to the initial values record from the fertilizer amended on the study area,
527 between +0.9 ‰ et +1.1 ‰ (Fig. 6).
528
529 **4.2.2 Input of nitrate undirect sources**
530
531 The $\delta^{15}N_{-NO3^-}$ values of crops (Fig. 6) vary between -1.9 ‰ and +1.3 ‰, and the $\delta^{18}O_{-NO3^-}$
532 values vary between +0.2 ‰ and +2.2 ‰, which is similar to values found in several
533 case studies (Panno et al. 2001; Mayer et al. 2002; Sebilo, 2003; Liu et al. 2006; Xue et al.
534 2009; Puig et al. 2013; Briand et al. 2017). Such low isotope ratios are typical for nitrate from
535 cultivated soils that have been intensely amended with synthetic fertilizers having $\delta^{15}N_{-N}$
536 values near 0 ‰ (Mariotti, 1982). The low $\delta^{18}O_{-NO3^-}$ values indicate that cultivated soil nitrate
537 is derived from the mineralization of soil organic matter and subsequent nitrification of
538 nitrogen based mineral fertilizers.
539
540 Nitrate concentrations of sewage effluents can vary, depending on the progress of the
541 treatment process. Indeed, in 22/03/2017 and 18/11/2017 samples, nitrate concentrations
542 were high, namely between 169.9 mg L^{-1} and 179.7 mg L^{-1}, respectively. NO_2^- and NH_4^+
543 concentrations also varied, illustrating the progress of the treatment process.
544 The isotopic values of derived effluents ranged between -1.9 ‰ and +6.3 ‰ for $\delta^{15}N$,
545 and between -4.8 ‰ and -2.1 ‰ for $\delta^{18}O$. Depending on the degree of volatilization and
546 nitrification during the treatment process, the output signal can vary.
547
548 The $\delta^{15}N_{-NO3^-}$ and $\delta^{18}O_{-NO3^-}$ values are significantly higher in soil amended with sewage
549 sludge, between +10.9 ‰ and +33.8 ‰ respectively for $\delta^{15}N_{-NO3^-}$, and between +27.0 ‰ and
550 +57.5 ‰ respectively for $\delta^{18}O_{-NO3^-}$. The spreading treatment process is based on nitrification-

551 denitrification cycles. These enriched isotopic compositions are typical for nitrate that has
552 undergone nitrification and partial denitrification during the treatment process (Kendall and
553 McDonnell, 1998; Derse et al. 2007).

554 After sewage sludge application to soils, another cycle of nitrification-denitrification
555 process occurs, leading to high $\delta^{15}N_{-NO3^-}$ and $\delta^{18}O_{-NO3^-}$ values. Hence, depending both on
556 treatment process and on soil biogeochemical, a sewage sludge source can have a very broad
557 range of values, as illustrated by Fig. 6.

558

559 **4.3 Nitrate isotopes for characterization of nitrate sources in both surface**
560 **water and groundwater in karst watershed**

561

562 The isotope compositions of nitrate in both surface waters and groundwaters are plotted
563 in Fig. 7A, Fig. 8A and Fig. 9 and compared with the isotope compositions of potential
564 source of nitrate. 0.5 slope arrows are plotted at the corners of potential sources to extend the
565 zone corresponding to the initial nitrate source.

566

567 **4.3.1 Endmembers of surface nitrate**

568

569 It is well known in karstic systems that surface water could directly contribute to spring
570 discharge by infiltration of water from temporary/occasional sinkholes in rivers (Rey et al.
571 2006; Huneau et al. 2013; Cholet et al. 2018; Lorette et al. 2021). The identification of nitrate
572 sources in surface waters is therefore a crucial prerequisite for a more general understanding
573 of the nitrogen dynamic at the catchment scale.

Fig. 7A is a magnification of the usual $\delta^{15}N_{vs}\delta^{18}O$ diagram focusing on two main nitrate potential sources: (i) NO_3^- from cultivated soil; (ii) NO_3^- from sewage. According to this figure, it is now considered that nitrate does not come from direct inputs such as atmospheric deposition or fertilizers, but rather from indirect input after biogeochemical transformation.

The isotopic compositions of nitrate ($\delta^{15}N$ and $\delta^{18}O$) for the Beauronne River and the Foncroze River seem to reflect the origin of cultivated soil that would have undergone partial denitrification, leading the nitrate in these waters having higher isotopic signatures both in $\delta^{15}N$ and $\delta^{18}O$. The highest $\delta^{15}N_{\text{-}NO3^-}$ and $\delta^{18}O_{\text{-}NO3^-}$ values, associated with water which has lower concentrations of nitrate, are measured in low-water conditions (LWC) (Fig. 7B), while the less enriched values of $\delta^{15}N_{\text{-}NO3^-}$ and $\delta^{18}O_{\text{-}NO3^-}$ are measured in high-water conditions (HWC), and are associated with water which has higher nitrate concentrations. Nitrate from soils, more depleted in $\delta^{15}N_{\text{-}NO3^-}$ and $\delta^{18}O_{\text{-}NO3^-}$ is exported into surface water during rainfall events.

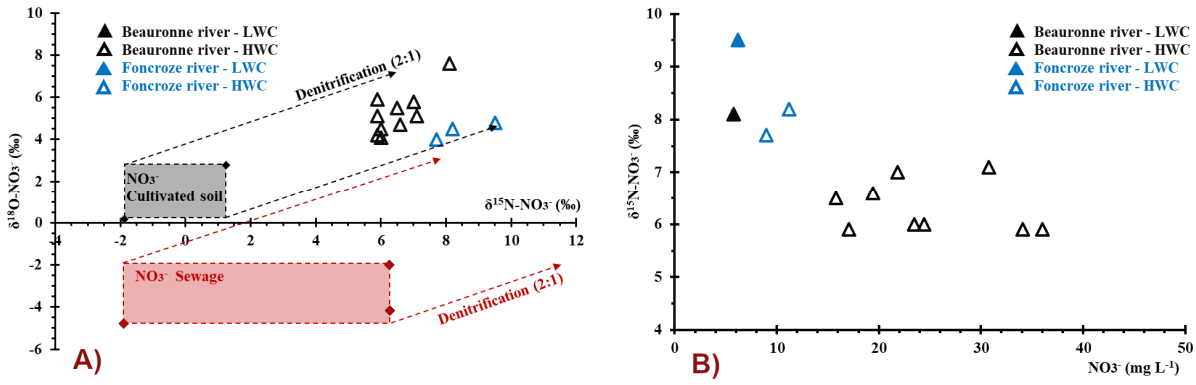

Fig. 7 : (A) $\delta^{15}N_{\text{-}NO3^-}$ vs $\delta^{18}O_{\text{-}NO3^-}$ measured in the Beauronne river and the Foncroze river. (B) NO_3^- vs $\delta^{15}N_{\text{-}NO3^-}$ measured in the Beauronne river and the Foncroze river. LWC : low-water condition. HWC : high-water condition.

4.3.2 Origins of groundwater nitrate

595 Groundwater data are plotted in Fig. 8A. Data are separated into: (i) springs located in
596 rural areas, (ii) springs located in urban areas.
597 For springs located in rural areas, nitrate records are from the mineralization of
598 synthetic N fertilizer mineralized in cultivated soil, according to NO_3^- isotopic compositions
599 (Fig. 8A). A denitrification process is identified according to the alignment of points on a
600 straight 0.5 slope line. Most enriched values have been recorded during low water conditions
601 (Fig. 8A), and the most depleted have been recorded during floods (Fig. 8A). Soil nitrate of
602 lower isotope composition enters groundwater during rainfall events. January 2016 flood
603 water had $\delta^{18}O_{\text{-}NO3^-}$ values which were more depleted than the expected theoretical minimum
604 $\delta^{18}O_{\text{-}NO3^-}$ values (+4.0 ‰), illustrating a possible quickflow component from the recharge to
605 the outlet from several springs.
606 Concerning springs located in urban areas, other isotope compositions of groundwater
607 nitrate are identified (Fig. 8A), implying another nitrate source. The nitrate isotope
608 concentrations of sewage effluent recorded in springs located in urban areas. As previously, a
609 denitrification process occurs.
610 Most springs have the same nitrate sources depending on hydrological situation. Two
611 springs show contamination from several sources: GW9 (Roche Pontissac springs) and
612 GW10 (Fontamiel spring). During low water conditions, $\delta^{15}N_{\text{-}NO3^-}$ and $\delta^{18}O_{\text{-}NO3^-}$ values of
613 GW10 are influenced by “Cultivated soil” type values (Fig. 8A). On the contrary, during high
614 water conditions, nitrate isotopes values change, and the origins suggest “Sewage” type
615 values. Similar observations were made for GW9 during the January 2016 flood event,
616 isotopic compositions of $\delta^{15}N_{\text{-}NO3^-}$ and $\delta^{18}O_{\text{-}NO3^-}$ show the influence of “Sewage” type values,
617 while during May 2016 flood event, these isotopic compositions are closer to those
618 associated with “Cultivated soil” type values (Fig. 8A). These observations confirm the

619 multiple sources that can be measured in the aquifer, and the potential mixtures that can
620 occur in a higher aquifer.
621
622 The chemical behavior of chloride (Cl^-) in natural waters is relatively conservative
623 because it is not subject to physical, chemical, or biological processes. The NO_3^- / Cl^- ratio
624 has been used for decades to highlight phenomena of mixtures or biological processes
625 responsible for the distribution of nitrate concentrations (Mengis et al. 1999; Vitoria et al.
626 2004; Li et al. 2013). Chemical synthetic N fertilizers are usually characterized by high
627 nitrogen and low chloride content. Domestic and animal effluents, on the contrary, have
628 higher Cl^- concentrations and lower NO_3^- / Cl^- ratios (Liu et al. 2006; Li et al. 2013). The
629 NO_3^- / Cl^- ratio decreases in the event of denitrification or consumption of the nitrates
630 without modifying the chloride concentrations. Fig. 8B confirms the results demonstrated by
631 comparison of nitrate isotopes compositions (Fig. 8A). Indeed, samples located in the bottom
632 right-hand part of Fig. 8B will characterize contamination by nitrate from domestic waste
633 ("Sewage" type values), while samples located in the left part of the graph suggest nitrate
634 origins from synthetic mineral fertilizers ("Cultivated soil" type values).
635 The observations made on Pontissac spring (GW 9) and Fontamiel spring (GW10) are
636 also made in Fig. 8B. For GW 9, the sample taken during the January 2016 flood event was
637 close to "Sewage" type values as is highlighted in Fig. 8A. On the contrary, the sample from
638 May 2016 is closer to the "Cultivated soil" type values. The findings are similar for GW10,
639 with water quality that changes over the hydrological cycle. During low water conditions, the
640 main signature seems to be synthetic N fertilizers, while it evolved towards signatures of
641 domestic wastes in January 2016 and May 2016.

The observation of data in NO_3^-/Cl^- vs Cl^- diagram consolidates the validity of the use of nitrate isotopes to identify the origins of nitrogen contamination in both surface and groundwater environments.

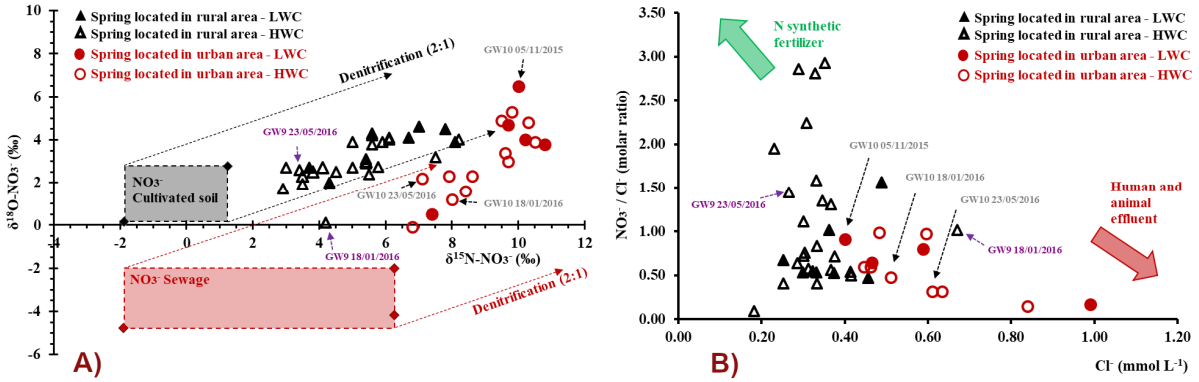

Fig. 8 : (A) $\delta^{15}N_{-NO3^-}$ vs $\delta^{18}O_{-NO3^-}$ measured in springs located over Toulon Springs hydrogeological catchment. (B) Cl^- vs NO_3^--Cl^- ratio measured in springs located over Toulon Springs hydrogeological catchment. LWC : low-water condition. HWC : high-water condition.

4.4 Nitrate sources and fate in the Toulon multilayered karst aquifer

Contrary to the springs described above, the Toulon Springs (GW1), which are the most important outlet of the study area, probably include all the nitrate isotopic signatures measured within the hydrogeological catchment. However, Fig. 9 reveals that the nitrate isotopes measured at the outlet are predominantly influenced by synthetic N fertilizers mineralized in cultivated soils. No linear relationship between $\delta^{15}N_{-NO3^-}$ and discharge (or water condition) is highlighted. The difficulty to interpret the isotope compositions of the Toulon Springs nitrate is probably associated with the complex infiltration process over the hydrogeological catchment, the various isotope compositions of the nitrate sources, and the various contribution rate of both Jurassic and upper Cretaceous aquifers (Lorette et al. 2018). The shift of points on the right-hand side of the graph, which follow a 0.5 slope line of,

highlights the high or low extent of the denitrification process. The other sources, such as septic effluents or sewage sludge, do not seem to influence the global signal at the outlet of the karst system, but are probably present in lower proportions.

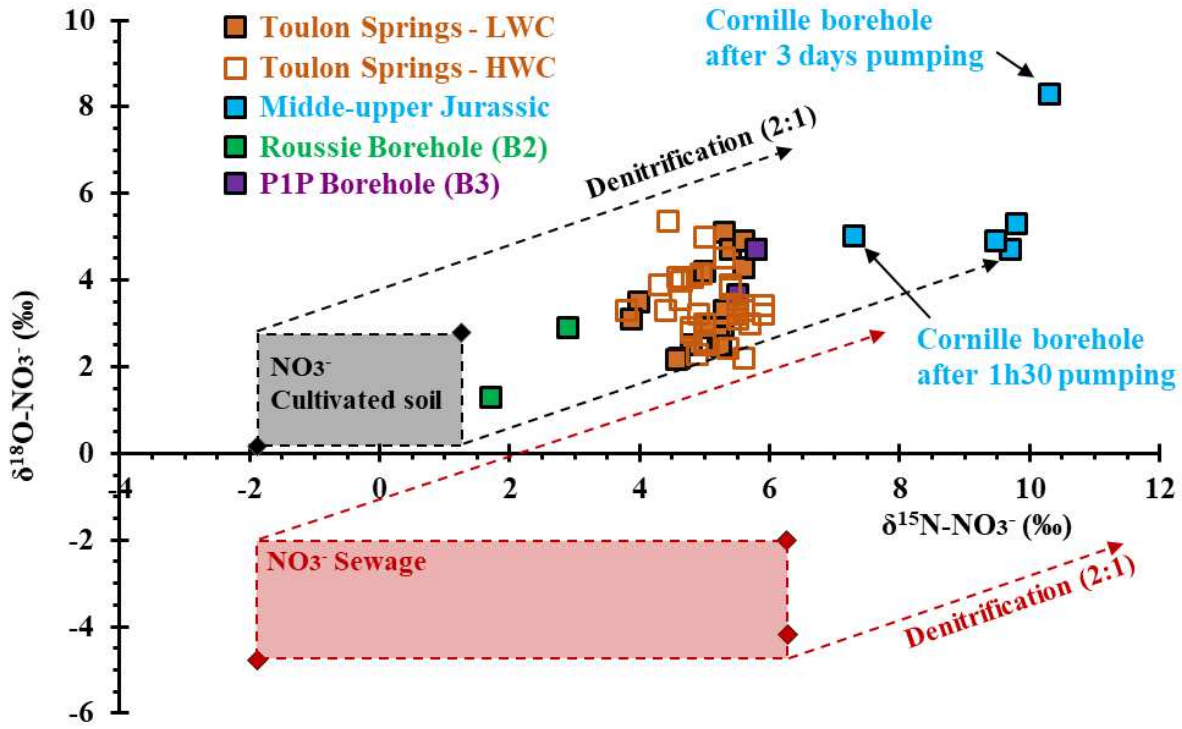

Fig. 9 : $\delta^{15}N_{-NO_3^-}$ and $\delta^{18}O_{-NO_3^-}$ measured in the Toulon Springs and boreholes over the study area. LWC : low-water condition. HWC : high-water condition.

Waters from the Cretaceous aquifer at Roussie borehole (B2) have nitrate isotope compositions from the same source as the Toulon Springs (Fig. 9). Proximity to the nitrate source in Fig. 9 indicates the low denitrification process of nitrate in water.

Water from the Jurassic confined aquifer at Cornille borehole (B1) is very important for the study area. As a reminder, B1 is a mix of the upper Cretaceous aquifer (Turonian) and upper Jurassic aquifer (Oxfordian, Kimmeridgian). The two samples taken in B1 were not obtained under the same conditions. 05/11/2015 sample was obtained after 1h30 of pumping. The geochemical facies of the water was characteristic of a mix between the two aquifers,

679 with dissolved oxygen concentration, magnesium concentration, and nitrate concentration of
680 2.29 mg L^{-1}, 5.69 mg L^{-1} and 13.14 mg L^{-1} respectively. The 18/09/2017 sample was obtained
681 after three days of pumping. The water geochemical facies was characteristic of the upper
682 Jurassic aquifer, with dissolved oxygen concentration, magnesium concentration, and nitrate
683 concentrations of 1.21 mg L^{-1}, 21.12 mg L^{-1} and 1.32 mg L^{-1} respectively. Nitrate isotopes
684 compositions for these two samples are from the same source ("Cultivated soil" type values)
685 but have different signatures. The $\delta^{15}N_{-NO3^-}$ and $\delta^{18}O_{-NO3^-}$ values of the samples containing
686 more upper Cretaceous water (05/11/2015) are more depleted than those samples with more
687 upper Jurassic water (18/09/2017) (Fig. 9).

688 The nitrate isotope composition of water from the mix between the two aquifers is
689 similar to that found for the Toulon Springs, as illustrated by the P1P borehole (B3) located
690 on the Toulon pumping plant site. This confirms previous studies demonstrating that the
691 Toulon Springs are fed by a multilayered karst aquifer from both an unconfined upper
692 Cretaceous karst aquifer and a confined Jurassic karst aquifer (Lastennet et al. 2004; Lorette
693 et al. 2017, 2018).

694 Results from the Cornille borehole (B1) are very important to understand the
695 hydrogeological functioning of the Toulon Springs hydrogeological catchment. Even though
696 the water is dated at about 2 800 years old in the upper Jurassic aquifer (unpublished data),
697 the $\delta^{15}N$ and $\delta^{18}O$ values of NO_3^- highlighted the impact of synthetic N fertilizers which have
698 been applied for several decades. The common origin of the nitrate found in the upper
699 Cretaceous and in the upper Jurassic still puts a question mark on the impermeable capacity
700 of the Cenomanian marls and hence on the protective captivity in the upper Jurassic. It is
701 highly probable that nitrate found in the upper Jurassic comes directly from the upper
702 Cretaceous.
703

According to the previous results of the main Toulon project, from Lorette et al. (2017, 2018, 2020), and Lorette (2019), a conceptual diagram of the hydrogeochemical functioning of the Toulon multilayered karst system associated with nitrogen transport is developped (Fig. 10).

It integrates direct sources of nitrogen (amount and isotopic values), and processes inducing changes in nitrate concentration within the soil before reaching the groundwater (detailed in the Fig. 4): (i) the different potential sources and a quantitative estimation of nitrogen input and output, (ii) the denitrification process occurring in both the Cretaceous karst aquifer (low denitrification), and in the upper Jurassic karst aquifer (high denitrification), (iii) the mix between the aquifers at the Toulon Springs.

Fig. 10A is a schematic N transformation occuring in the soil according to the land use over the Toulon Springs hydrogeological catchment, where different N input are suggested. It distinguishes "N applied" and "NO_3^- infiltrated". N applied describe the identified and quantified N potential sources over the hydrogeological catchment. The quantitative annual estimation is that 349 T $year^{-1}$ of nitrogen input come from N synthetic fertilizer, whereas 9 T $year^{-1}$ and 8 T $year^{-1}$ come from spreading sludge and sewage respectively. Finally, 49 T $year^{-1}$ of nitrogen input comes from rainfall, but almost the entire quantity is attenuated in the soil (Katz et al. 2009; Lombardo Associates, 2011). NO_3^- infiltrated describe the derived nitrate which can leak to the aquifer after a number of factors which appear into the soil, such as: (i) the use of nitrogen by plants for their growth; and (ii) the partial denitrification process which occurs in the soil and in the saturated zone of the aquifer. Hence, these several factors act to decrease the quantity of NO_3^- infiltrated compared to N applied over the surface.

Concerning isotopic composition, Fig. 10A show than $\delta^{15}N_{\text{-}NO3}^-$ from potential sources (or N applied) are different than $\delta^{15}N_{\text{-}NO3}^-$ from NO_3^- infiltrated (or undirect sources as

729 explain previously in Fig.4 and also in sections 3.4, 4.2.1, and 4.2.2). Hence, the mix of every
730 undirect sources implies the $\delta^{15}N_{-NO3^-}$ signature of the upper part of the Toulon karst aquifer
731 (upper Cretaceous with low denitrification during short time period).

732 At the outlet of the Toulon karst system, annual nitrogen outputs are similar despite
733 differences in the total volume recorded. About 40 TN $year^{-1}$ have been recorded at the outlet
734 (Fig. 10B). The $\delta^{15}N_{-NO3^-}$ recorded (+4.5 ‰) is hence a mix between $\delta^{15}N_{-NO3^-}$ from
735 Cretaceous unconfined karst aquifer (+2.5 ‰) and $\delta^{15}N_{-NO3^-}$ from Jurassic confined karst
736 aquifer (+10.0 ‰), depending hydrogeological conditions and quick flow component.
737

738 **4.5 Implication for water management and vulnerability of the Toulon**
739 **multilayer karst system**
740

741 Over the Toulon Springs hydrogeological catchment, land use associated with the karst
742 landscape entails specific water management. Geomorphological features such as sinkholes
743 or swallowholes imply a potential direct and rapid transfer of any contaminant from the
744 surface to the outlet.

745 The Toulon Springs are a strategic resource for drinking water in Dordogne. The
746 increasing trend of nitrate concentration in the Toulon Springs (Fig. 2), means that a specific
747 methodology to characterize the vulnerability to nitrate contamination in the multilayer karst
748 system has to be developed. These results have implications for water management in that
749 they provide a better quantification of nitrate input in surface. For cropland, the survey must
750 focus on: (i) the use of karst landscapes for cropland, (ii) decreasing anthropogenic nitrogen
751 input such as synthetic N fertilizer to minimize the leaching of nitrate to the underlying
752 aquifer. For urban areas, the construction of new residential neighborhoods must be sensitive
753 to the constraints of the karst environment.

754 In terms of vulnerability, the Cretaceous unconfined multilayer karst aquifer has a low
755 denitrification capacity as highlighted by the isotope composition of nitrate. This means that
756 this resource is directly vulnerable to surface pollution. Over the Toulon multilayered karst
757 system, complex hydrogeological relationships between aquifers (Lorette et al. 2018) allow
758 nitrate transfer from the upper Cretaceous unconfined aquifer to the upper Jurassic confined
759 aquifer. Intense denitrification processes associated with long residence times and anoxic
760 water make the upper Jurassic karst aquifer less vulnerable to surface pollution. However, a
761 water quality survey is necessary in order to avoid the increase of nitrate concentrations in
762 the future. This study on nitrate isotopes has shown that although the upper Jurassic aquifer
763 seems less vulnerable than the upper Cretaceous aquifer, water from the upper Cretaceous
764 can nonetheless infiltrate into the upper Jurassic aquifer through the Cenomanian marls.
765 Thus, the idea that the upper Jurassic aquifer has a protective role would be wrong, implying
766 that deeper drilling is needed to capture waters from the middle Jurassic.
767 No nitrate concentrations were recorded for the middle Jurassic aquifer, testifying to
768 the good natural protection of the aquifer. However, particular attention must be paid to this
769 aquifer. For the past 25 years an increasing number of boreholes have been drilled through
770 this aquifer for drinking water or industries (Lorette, 2019), and its possible over-exploitation
771 could be dangerous for its still protected quality and could lead to a downward infiltration.
772 Consequently, local public health organizations should also extensively monitor the water by
773 to ensure that the water quality in the middle Jurassic is maintained.
774

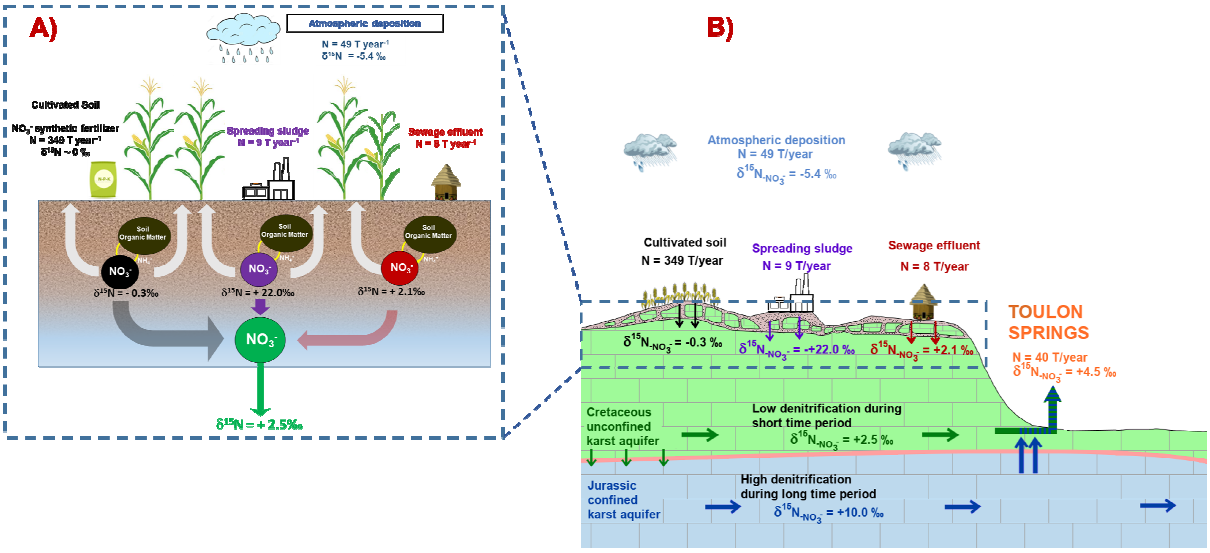

Fig. 10 : (A) Schematic N transformation occuring in the soil over the Toulon Springs hydrogeological catchment (B) Conceptual model of the functioning of Toulon karst system associated with nitrogen transfer and quantitative estimation of nitrogen fluxes.

5. Conclusion

In water management, it is important to know nitrate sources. In this research, an approach for tracing nitrate sources in multilayered karst aquifers has been proposed. First, the approach involves the identification of water type and nitrate concentrations over the hydrogeological catchment, in both surface water and groundwater. The second step consists of analyzing every potential source of nitrate over the study area using nitrate isotopes ($\delta^{15}N$ and $\delta^{18}O$). The third step consists of linking nitrate isotopic compositions of surface water and groundwater, to those of potential sources of nitrate. Biogeochemical processes in the N cycle, such as nitrification or denitrification, are integrated into the planning process to identify nitrate sources in the study area. The final step consists of integrating isotopic values in the hydrogeological context to evaluate the fate of nitrate in multilayered karst aquifer, in order to propose better water management.

The approach was applied on a major karst system in western France: the Toulon system. Results showed two main nitrate sources: (i) N synthetic fertilizers (ammonium nitrate) mineralized in cultivated soils and (ii) sewage effluents. Both of these nitrate sources underwent more or less denitrification before reaching the sampling points. Within the Toulon Springs hydrogeological catchment, surface waters are contaminated with nitrate from N synthetic fertilizer (primary source) mineralized in cultivated soils (secondary source). Most of the springs in the catchment are also contaminated with this nitrate source, but some indicate nitrate isotope composition of sewage effluent origin. Finally, the Toulon Springs are only contaminated with nitrate from N synthetic fertilizer mineralized in cultivated soils.

This work highlights soil properties in changing N direct isotopic compositions. Hence, to have a better idea of nitrate sources affecting surface water or groundwater, a knowledge of nitrate isotopic compositions of is fundamental. This research suggests discussion about the fate of nitrate in a karst system with complex hydrogeological relationships. This work has showed the potential use of nitrate isotopes as a tool for characterization of the functioning in a multilayered karst aquifer. Over the Toulon Springs hydrogeological catchment, this work on nitrate isotopes has showed that water from the upper Cretaceous layers can infiltrate the upper Jurassic aquifer through the Cenomanian marls. This new result on the study area highlights the value of this work in water management and the vulnerability of water quality in karst environments. The study on the purifying properties which aquifers have on nitrate contamination, offers good perspectives for better water management in karst environments.

From a more fundamental standpoint, this work provides a set of parameters adapted for a karstic hydrogeological catchment. Future steps of this research will provide a common

817 approach for karst environments, focusing on N transformation of primary sources in soil and
818 consequences on nitrate isotopic compositions, within contrasted karst catchments.
819 This methodology, based on the combination of both nitrate isotope and
820 hydrogeological tools, provides new information about nitrate sources and fate in karst
821 environments, and gives tools for implementation of remediation measures to protect the
822 water resources. The innovative way of implementing the method should encourage its use in
823 other karst aquifers with similar issues, and hence, lead to an easy method of comparison
824 between karst systems.
825

826 **Acknowledgements**

827 This work was supported by the Région Aquitaine, the city of Périgueux, Suez, the
828 Conseil Général de la Dordogne, and the Adour-Garonne Water Agency. The authors thank
829 Suez's agents for the technical assistance and the field knowledge they contributed. They
830 finally want to thank Dr. David VIENNET for his help in proof reading the article.
831 This work benefited from fruitful discussion within the French network of karst
832 observatories (SNO Karst), initiative from the INSU/CNRS.
833

834 **Supplementary information**
835

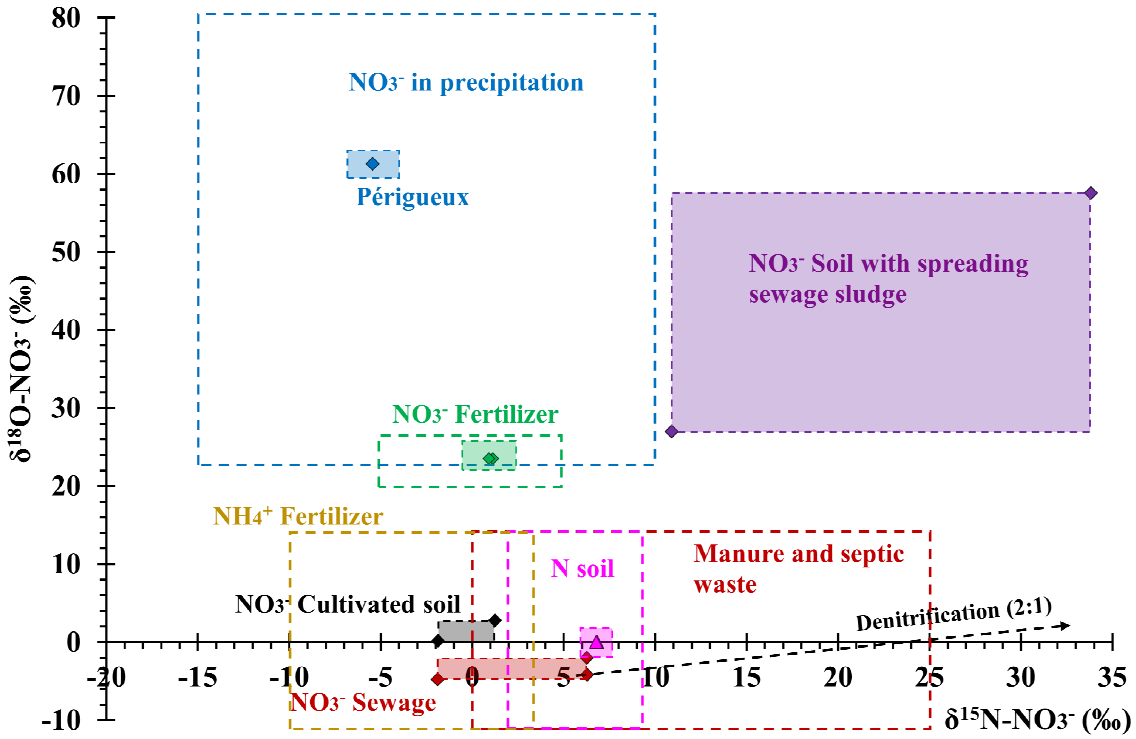

836

837 **Kendall plot vs data obtained from the hydrogeological catchment. Empty rectangles are from Kendall et**

838 **al. 2007. Full rectangles with points are from this study.**

839

840

841

Sample description, chemical composition (mg L^{-1}) and isotopic composition (‰) of groundwater samples.

Sample designation	Sample name	Date	Aquifer	T (°C)	pH (pH unit)	EC (µS cm^{-1})	O_2 (mg L^{-1})	Ca^{2+} (mg L^{-1})	Mg^{2+} (mg L^{-1})	Na^{+} (mg L^{-1})	K^{+} (mg L^{-1})	HCO_3^- (mg L^{-1})	Cl^- (mg L^{-1})	SO_4^{2-} (mg L^{-1})	NO_3^- (mg L^{-1})	SiO_2 (mg L^{-1})	$\delta^{18}O_{-H2O}$ (‰)	$\delta^{15}N_{-NO3^-}$ (‰)	$\delta^{18}O_{-NO3^-}$ (‰)	Balance (%)
Monzie spring	GW 2	03/11/2015	Cretaceous	13.3	7.0	675	8.6	139.0	3.1	9.8	1.0	396.5	16.0	16.2	13.4	14.5	-6.3	8.1	3.9	1.0
Monzie spring	GW 2	19/01/2016	Cretaceous	13.2	7.0	620	9.0	124.1	2.9	9.4	1.3	342.8	14.5	16.6	12.8	12.8	-6.3	7.5	3.2	2.3
Monzie spring	GW 2	23/05/2016	Cretaceous	13.2	7.1	645	9.4	135.5	3.2	9.5	1.4	364.8	14.5	21.2	13.8	12.6	-6.0	8.2	4.0	3.0
Abbay spring	GW 3	19/01/2016	Cretaceous	12.8	7.0	643	9.5	136.5	2.5	10.9	0.9	378.2	15.5	16.2	18.7	17.2	-	9.7	3.0	2.1
Abbay spring	GW 3	25/05/2016	Cretaceous	12.7	6.9	651	9.1	122.9	2.2	9.8	0.8	388.0	14.5	11.9	13.1	17.3	-	9.6	3.4	-3.4
Lavaure spring	GW 4	03/11/2015	Cretaceous	12.9	7.4	442	10.0	84.5	2.4	9.2	0.9	252.5	13.1	6.2	12.2	14.5	-5.8	5.4	3.1	0.1
Lavaure spring	GW 4	18/01/2016	Cretaceous	12.7	7.6	419	10.1	80.0	2.5	8.2	1.1	209.8	11.7	9.2	17.2	13.2	-6.4	5.4	2.9	4.0
Lavaure spring	GW 4	25/05/2016	Cretaceous	12.6	7.4	456	10.2	79.0	2.3	8.9	0.9	249.3	12.8	6.7	12.8	14.3	-6.1	5.9	3.9	-2.6
Rouchou spring	GW 5	03/11/2015	Cretaceous	13.8	7.1	563	7.3	118.7	2.5	7.1	0.9	357.5	10.5	6.0	9.8	17.6	-	4.3	2.0	0.3
Rouchou spring	GW 5	18/01/2016	Cretaceous	13.2	7.0	590	7.9	119.4	2.4	6.9	1.1	355.0	10.0	6.0	11.3	14.8	-	4.1	2.7	0.7
Rouchou spring	GW 5	25/05/2016	Cretaceous	13.1	6.9	596	7.4	111.0	2.5	7.1	0.8	339.2	11.6	7.7	8.3	14.3	-	5.4	3.0	-0.8
Godet spring	GW 6	03/11/2015	Cretaceous	12.5	6.9	600	8.0	124.1	2.7	8.0	1.3	359.9	11.6	9.0	10.9	17.9	-6.4	7.0	4.6	1.8
Godet spring	GW 6	19/01/2016	Cretaceous	12.4	6.8	562	7.6	112.2	2.6	8.1	1.2	313.5	10.6	10.8	14.3	15.1	-6.3	4.5	2.5	3.1
Godet spring	GW 6	23/05/2016	Cretaceous	12.1	6.9	442	8.0	81.8	1.9	6.3	0.9	259.9	8.8	8.2	6.3	13.0	-6.0	6.1	4.1	-2.5
Bayolle spring	GW 7	04/11/2015	Cretaceous	14.9	7.4	620	7.6	122.2	3.4	8.4	3.6	323.3	17.1	12.8	47.4	15.9	-	7.8	4.5	0.3
Bayolle spring	GW 7	18/01/2016	Cretaceous	12.4	6.9	601	8.1	116.2	2.4	7.3	1.6	301.3	11.5	9.3	57.3	16.5	-	5.5	2.4	-0.1
Bayolle spring	GW 7	23/05/2016	Cretaceous	12.3	6.9	605	7.4	114.6	2.5	7.7	0.9	318.4	12.8	9.5	29.8	16.9	-	5.6	4.2	0.3
Bezan spring	GW 8	04/11/2015	Cretaceous	13.7	7.0	655	8.9	136.4	2.7	7.9	2.5	372.1	12.7	9.1	22.7	22.4	-	6.7	4.1	3.1
Bezan spring	GW 8	18/01/2016	Cretaceous	13.0	7.0	637	8.1	136.2	1.9	6.2	1.6	356.2	10.1	9.9	51.3	19.0	-	3.8	2.5	0.8
Bezan spring	GW 8	23/05/2016	Cretaceous	12.8	6.9	585	7.9	110.3	1.7	4.9	1.0	325.7	8.1	8.3	27.9	17.7	-	3.5	2.3	-2.4
Roche Pontissac spring	GW 9	18/01/2016	Cretaceous	13.0	7.0	646	6.1	137.6	2.0	5.8	2.2	362.3	23.5	7.9	42.2	12.8	-	4.2	2.1	1.3
Roche Pontissac spring	GW 9	23/05/2016	Cretaceous	12.1	7.0	589	6.7	113.0	1.7	4.6	0.7	320.9	9.3	6.8	23.8	11.2	-	3.4	2.6	-0.3
Fontamiel spring	GW 10	05/11/2015	Cretaceous	13.7	7.1	540	9.0	102.4	2.4	10.1	1.6	301.3	14.0	4.5	22.7	10.4	-	10.0	6.5	0.1
Fontamiel spring	GW 10	18/01/2016	Cretaceous	12.6	7.7	482	9.8	89.4	2.1	12.5	1.4	264.7	17.9	6.7	15.1	8.6	-	8.0	4.2	-0.1
Fontamiel spring	GW 10	23/05/2016	Cretaceous	12.5	7.1	495	9.7	82.0	1.9	16.5	1.2	258.6	21.4	6.9	12.0	8.3	-	7.1	3.3	-1.7
Fongou spring	GW 11	18/01/2016	Cretaceous	12.6	6.9	686	6.1	145.2	2.1	7.3	0.7	372.1	12.3	4.7	64.1	7.6	-	5.8	2.7	-1.3
Fongou spring	GW 11	23/05/2016	Cretaceous	12.5	6.8	662	5.6	130.3	1.8	6.6	1.4	337.5	10.8	5.8	42.8	6.7	-	6.1	4.0	-2.5
Bories spring	GW 12	04/11/2015	Cretaceous - Jurassic	14.1	7.1	558	5.9	105.1	10.2	4.9	0.8	341.6	8.8	6.5	10.5	7.4	-	3.7	2.7	1.6
Bories spring	GW 12	20/01/2016	Cretaceous - Jurassic	13.0	7.0	548	6.6	106.3	5.7	6.5	0.9	312.3	10.5	7.5	13.5	11.6	-	5.0	2.7	2.9
Bories spring	GW 12	24/05/2016	Cretaceous - Jurassic	13.4	7.1	598	5.9	105.3	6.9	6.1	0.9	340.4	10.9	7.2	11.2	10.7	-	5.6	3.8	-0.7
Antonne spring	GW 13	04/11/2015	Cretaceous	14.7	7.2	696	6.2	130.4	3.7	16.1	7.2	374.5	34.7	11.8	10.4	16.7	-	7.4	0.5	1.2
Antonne spring	GW 13	20/01/2016	Cretaceous	13.6	7.2	615	6.5	113.4	3.0	17.4	7.2	327.0	29.4	11.4	7.7	16.8	-	6.8	-0.1	2.4
Antonne spring	GW 13	24/05/2016	Cretaceous	13.4	7.2	638	8.5	108.4	3.2	15.6	5.9	353.8	22.2	11.4	12.5	14.8	-	7.9	2.3	-2.6
Clavelie spring	GW 14	04/11/2015	Cretaceous	14.2	7.0	646	2.9	124.4	5.5	6.7	1.0	368.4	11.3	8.4	11.0	23.1	-6.3	5.6	4.3	2.2
Clavelie spring	GW 14	19/01/2016	Cretaceous	13.4	6.9	572	6.8	115.5	2.1	6.3	0.9	322.1	12.1	11.2	28.9	22.5	-6.4	3.5	1.9	-0.2
Clavelie spring	GW 14	24/05/2016	Cretaceous	13.5	7.0	660	4.9	124.5	3.5	7.0	1.0	363.6	13.1	9.3	16.7	21.9	-6.1	5.0	3.9	0.4
Malades spring	GW 15	04/11/2015	Cretaceous	14.4	7.1	643	7.4	126.0	3.4	13.2	2.0	329.4	20.6	23.1	28.9	14.1	-	10.2	4.0	2.0
Malades spring	GW 15	20/01/2016	Cretaceous	14.2	7.0	653	7.9	127.0	3.7	15.4	2.4	324.5	20.8	26.7	35.9	14.2	-	8.6	2.3	2.4
Malades spring	GW 15	24/05/2016	Cretaceous	14.0	7.0	621	7.4	105.6	3.2	13.0	2.2	329.4	16.9	24.4	29.5	12.8	-	8.4	1.6	-5.3
CAP spring	GW 16	04/11/2015	Cretaceous - Jurassic	19.0	7.1	640	4.4	93.4	20.0	10.7	2.0	364.8	16.3	13.2	18.5	14.2	-	10.8	3.8	-1.2
CAP spring	GW 16	19/01/2016	Cretaceous - Jurassic	18.6	7.1	618	3.4	89.5	19.8	11.3	1.6	333.1	16.2	11.5	17.1	14.0	-	10.5	3.9	1.7
CAP spring	GW 16	23/05/2016	Cretaceous - Jurassic	20.0	7.1	605	3.3	84.0	20.9	10.6	1.4	333.1	15.6	14.3	16.4	13.3	-	10.3	4.8	-0.2
COPO spring	GW 17	19/01/2016	Jurassic	20.4	7.2	530	1.5	80.5	22.7	8.0	1.0	325.7	12.5	11.0	8.5	14.4	-6.6	9.7	4.7	2.4
COPO spring	GW 17	24/05/2016	Jurassic	20.6	7.1	542	1.5	82.0	23.2	8.3	0.8	328.2	12.5	9.6	6.4	13.6	-6.6	9.5	4.9	3.1
COPO spring	GW 17	16/08/2016	Jurassic	20.4	7.2	555	1.6	82.5	21.5	8.0	0.8	333.6	12.7	8.4	7.2	13.4	-6.5	9.8	5.3	1.4

842

843

844 **Sample description, chemical composition (mg L^{-1}) and isotopic composition (‰) of surface water samples.**

Sample designation	Sample name	Date	T (°C)	pH (pH unit)	EC (µS cm^{-1})	O_2 (mg L^{-1})	Ca^{2+} (mg L^{-1})	Mg^{2+} (mg L^{-1})	Na^{+} (mg L^{-1})	K^{+} (mg L^{-1})	HCO_3^{-} (mg L^{-1})	Cl^{-} (mg L^{-1})	SO_4^{2-} (mg L^{-1})	NO_3^{-} (mg L^{-1})	SiO_2 (mg L^{-1})	$\delta^{18}O_{-H2O}$ (‰)	$\delta^{15}N_{-NO3}^{-}$ (‰)	$\delta^{18}O_{-NO3}^{-}$ (‰)	Balance (%)
Beauronne - Reymondens	SW 1	03/11/2015	11.9	7.7	566	4.3	109.4	3.3	11.2	3.7	334.3	16.9	5.6	5.8	14.9	-	8.1	7.6	1.3
Beauronne - le Cros	SW 2	25/01/2016	9.4	8.0	625	11.0	118.5	2.4	7.1	1.2	347.7	12.2	8.8	17.1	13.3	-	5.9	5.9	-0.3
Beauronne - Château l'Evêque	SW 3	25/01/2016	9.7	8.0	633	11.3	127.6	2.6	7.0	1.1	345.3	12.5	10.7	23.5	14.9	-	6.0	4.1	2.3
Beauronne - Château l'Evêque	SW 3	26/05/2016	14.7	7.9	594	10.2	114.6	2.3	5.8	1.0	318.4	10.1	8.3	15.8	14.0	-	6.5	5.5	2.2
Beauronne - Preyssac	SW 4	22/01/2016	7.4	8.0	639	11.0	127.4	2.3	6.8	1.2	341.6	12.1	11.2	30.8	15.3	-	7.1	5.1	1.6
Beauronne - Preyssac	SW 4	26/05/2016	14.1	7.8	605	9.8	116.9	2.2	5.8	1.0	334.3	10.2	8.8	19.4	13.7	-	6.6	4.7	0.3
Beauronne - Borie des Cailloux	SW 5	22/01/2016	8.1	8.0	646	10.5	129.1	2.2	6.9	1.2	342.8	12.4	11.7	34.1	14.9	-	5.9	5.1	1.5
Beauronne - Borie des Cailloux	SW 5	26/05/2016	14.1	7.8	613	9.6	115.8	2.3	5.9	1.1	330.6	10.7	9.0	21.8	13.3	-	7.0	5.8	0.0
Beauronne - Agonac	SW 6	22/01/2016	8.5	7.7	645	10.1	132.4	2.1	6.3	1.2	335.5	11.9	12.6	36.0	15.3	-	5.9	4.2	3.1
Beauronne - Agonac	SW 6	26/05/2016	14.1	7.6	617	9.9	115.8	2.3	5.9	1.1	328.2	10.9	9.6	24.4	13.1	-	6.0	4.5	-0.1
Foncroze - Monzie	SW 7	03/11/2015	14.4	7.8	616	7.1	126.3	2.8	10.2	1.7	364.8	15.3	12.6	6.2	14.1	-	9.5	4.8	1.9
Foncroze - Monzie	SW 7	22/01/2016	8.0	7.9	634	10.9	128.0	2.5	9.6	1.0	374.5	15.4	20.7	11.2	12.7	-	8.2	4.5	-0.9
Foncroze - Monzie	SW 7	26/05/2016	14.5	7.7	622	8.9	124.2	2.7	9.4	1.0	352.6	13.7	18.6	9.0	11.8	-	7.7	4.0	1.2

845

846

847

Sample description, chemical composition (mg L^{-1}) and isotopic composition (‰) of Toulon Springs samples (adapted from Lorette et al. 2018).

Sample designation	Sample name	Date	T (°C)	pH (pH unit)	EC (µS cm^{-1})	O_2 (mg L^{-1})	Ca^{2+} (mg L^{-1})	Mg^{2+} (mg L^{-1})	Na^{+} (mg L^{-1})	K^{+} (mg L^{-1})	HCO_3^- (mg L^{-1})	Cl^- (mg L^{-1})	SO_4^{2-} (mg L^{-1})	NO_3^- (mg L^{-1})	SiO_2 (mg L^{-1})	$\delta^{18}O_{-H2O}$ (‰)	$\delta^{15}N_{-NO3}^-$ (‰)	$\delta^{18}O_{-NO3}^-$ (‰)	Discharge (L s^{-1})	Balance (%)
Toulon Springs	GW 1	06/10/2015	14.4	7.0	594	4.1	104.5	11.9	6.5	1.1	344.0	10.8	8.6	10.6	13.6	-6.93	4.8	2.5	289	3.7
Toulon Springs	GW 1	20/10/2015	14.2	7.1	594	4.3	103.6	12.1	6.4	1.0	341.6	10.7	8.6	10.4	13.7	-7.05	4.0	3.5	286	3.8
Toulon Springs	GW 1	03/11/2015	14.2	7.0	593	4.3	101.9	12.2	6.2	0.9	342.8	11.0	8.3	10.6	13.5	-7.05	5.3	5.1	294	1.8
Toulon Springs	GW 1	25/11/2015	14.2	7.0	593	4.3	101.3	12.7	6.4	1.0	339.2	11.4	9.3	10.0	13.4	-7.26	5.0	4.2	302	3.5
Toulon Springs	GW 1	22/12/2015	14.4	7.1	586	4.3	100.8	12.6	6.4	1.1	347.7	10.8	9.3	10.6	12.7	-7.23	4.6	2.2	297	2.1
Toulon Springs	GW 1	30/12/2015	14.4	7.1	583	4.1	99.4	12.3	6.3	0.9	342.8	11.0	9.9	10.8	12.6	-7.09	3.9	3.1	281	1.8
Toulon Springs	GW 1	05/01/2016	14.4	7.1	586	4.0	99.3	12.4	6.9	0.7	348.9	11.0	9.9	10.8	12.1	-6.70	5.3	3.3	404	1.2
Toulon Springs	GW 1	08/01/2016	14.3	7.0	597	4.5	107.1	11.4	6.4	0.9	351.4	11.3	10.6	12.4	13.2	-	4.6	3.5	565	0.8
Toulon Springs	GW 1	11/01/2016	14.0	7.0	591	4.9	110.3	9.3	6.6	1.1	342.8	12.0	11.5	14.5	13.9	-	5.6	2.2	733	1.4
Toulon Springs	GW 1	12/01/2016	14.0	7.0	581	5.1	108.2	8.8	6.7	1.2	339.2	11.8	11.2	13.6	14.4	-7.16	5.7	3.0	763	1.0
Toulon Springs	GW 1	13/01/2016	13.8	7.0	574	5.6	107.8	7.9	6.8	1.2	316.0	11.7	11.1	14.8	14.5	-7.02	4.6	4.0	778	3.2
Toulon Springs	GW 1	14/01/2016	13.7	7.0	567	5.9	107.2	7.0	6.8	1.2	311.1	11.7	10.9	16.3	15.2	-7.07	5.6	3.3	751	2.9
Toulon Springs	GW 1	15/01/2016	13.6	7.0	559	6.3	108.4	6.0	6.6	1.3	309.9	11.3	10.5	16.4	15.2	-6.31	5.5	3.4	748	3.0
Toulon Springs	GW 1	18/01/2016	13.4	7.0	543	6.7	106.6	4.3	6.4	1.3	308.7	10.8	11.1	19.7	15.4	-5.87	4.6	4.1	709	0.7
Toulon Springs	GW 1	19/01/2016	13.4	7.0	546	6.7	108.9	4.1	7.3	1.3	309.9	10.8	11.4	19.0	15.6	-7.01	5.0	5.0	670	1.8
Toulon Springs	GW 1	22/01/2016	13.3	7.0	550	6.6	109.1	4.0	6.3	1.3	317.2	10.6	11.4	19.4	15.4	-7.31	4.8	2.9	635	0.5
Toulon Springs	GW 1	25/01/2016	13.3	7.0	574	6.6	110.3	4.4	6.2	1.2	320.9	10.9	11.0	18.1	15.5	-6.74	4.3	3.9	600	0.7
Toulon Springs	GW 1	27/01/2016	13.4	7.0	578	6.3	110.7	4.8	6.2	1.1	335.6	10.9	10.9	18.4	15.5	-7.00	5.4	3.8	560	-0.8
Toulon Springs	GW 1	29/01/2016	13.4	7.0	581	6.5	112.8	5.4	6.2	1.2	339.2	10.5	8.8	17.2	15.0	-7.19	5.0	2.5	557	0.5
Toulon Springs	GW 1	03/02/2016	13.7	7.0	600	6.0	113.8	6.4	6.2	1.2	351.4	11.4	9.5	16.9	15.3	-6.55	5.4	3.9	695	-0.2
Toulon Springs	GW 1	05/02/2016	13.5	7.0	598	6.1	112.8	6.5	6.4	1.2	342.8	11.1	9.4	17.0	15.1	-7.16	5.6	3.4	574	0.6
Toulon Springs	GW 1	09/02/2016	13.4	7.0	593	6.0	110.9	6.1	6.3	1.2	345.3	11.1	9.2	16.7	16.0	-7.09	4.8	4.1	695	-0.6
Toulon Springs	GW 1	11/02/2016	13.4	7.0	580	6.5	110.9	5.7	6.4	1.3	328.7	11.1	9.1	16.5	15.7	-7.10	4.8	2.8	831	1.4
Toulon Springs	GW 1	17/02/2016	13.1	7.0	515	6.9	105.0	3.5	6.0	1.3	295.8	10.4	8.7	14.7	16.7	-6.82	3.8	3.3	870	2.4
Toulon Springs	GW 1	24/02/2016	12.9	6.9	528	7.0	110.4	3.2	6.2	1.3	305.3	10.9	9.3	13.8	16.7	-7.21	5.3	4.5	779	3.0
Toulon Springs	GW 1	03/03/2016	13.1	6.9	557	6.3	109.8	4.4	6.1	1.1	321.8	10.8	8.7	13.0	17.1	-6.45	4.9	3.2	678	1.5
Toulon Springs	GW 1	09/03/2016	13.1	6.9	565	6.2	107.3	4.4	5.7	1.0	327.6	10.9	8.4	12.5	17.0	-6.91	4.4	5.4	755	-0.4
Toulon Springs	GW 1	16/03/2016	13.2	6.9	559	6.7	107.3	4.0	6.6	0.9	320.5	11.1	8.8	12.6	16.9	-6.31	5.5	3.1	707	0.4
Toulon Springs	GW 1	29/03/2016	13.4	7.0	582	5.7	110.1	5.7	6.6	0.7	338.9	11.3	9.0	12.1	17.3	-6.35	4.9	4.2	536	0.2
Toulon Springs	GW 1	06/04/2016	13.5	7.0	585	5.5	109.9	6.7	6.1	0.8	341.9	11.2	9.1	12.6	17.1	-6.87	5.0	3.0	516	0.2
Toulon Springs	GW 1	20/04/2016	13.5	6.9	571	5.8	106.9	5.6	5.9	1.0	332.8	11.0	9.0	11.5	16.5	-6.88	5.9	3.2	725	-0.4
Toulon Springs	GW 1	27/04/2016	13.2	6.9	568	6.4	106.7	4.0	5.7	1.0	334.5	10.8	9.1	11.3	17.1	-6.59	4.9	2.3	655	-1.8
Toulon Springs	GW 1	04/05/2016	13.4	6.9	580	5.9	107.9	5.9	5.7	0.9	345.6	11.0	9.0	11.2	16.9	-6.25	5.0	2.6	527	-1.5
Toulon Springs	GW 1	11/05/2016	13.5	6.9	594	5.8	108.3	6.5	5.9	0.8	355.4	11.2	9.1	11.8	16.5	-6.18	4.4	3.3	512	-2.2
Toulon Springs	GW 1	17/05/2016	13.7	6.9	598	5.2	104.3	7.9	6.4	0.9	356.1	11.3	9.0	11.8	16.5	-6.74	5.9	3.4	455	-2.8
Toulon Springs	GW 1	23/05/2016	13.8	7.0	600	5.1	106.3	8.3	6.5	0.9	346.5	11.1	9.1	12.2	16.1	-6.43	5.5	3.2	575	-0.5
Toulon Springs	GW 1	01/06/2016	13.6	6.9	577	5.2	104.9	7.2	6.7	1.0	339.0	11.4	9.2	12.2	16.3	-6.53	5.4	2.4	544	-0.8
Toulon Springs	GW 1	07/06/2016	13.6	7.0	576	5.3	112.8	7.0	6.4	1.0	330.6	10.7	9.1	12.2	16.1	-6.39	5.5	3.4	504	3.3
Toulon Springs	GW 1	21/06/2016	13.6	7.0	580	5.1	103.6	7.4	6.4	1.0	344.7	10.4	8.0	11.7	15.3	-6.41	5.4	4.7	573	-1.6
Toulon Springs	GW 1	29/06/2016	13.6	7.0	579	5.4	106.0	7.1	6.4	1.0	349.7	10.3	8.0	11.7	15.7	-6.42	5.3	2.9	472	-1.4
Toulon Springs	GW 1	13/07/2016	13.8	6.9	587	4.7	105.9	8.4	6.1	0.8	352.6	10.7	7.4	12.6	15.8	-6.14	5.5	3.2	417	-1.2
Toulon Springs	GW 1	20/07/2016	13.9	7.0	591	4.7	104.5	8.8	6.4	0.7	352.0	10.6	7.4	12.7	15.5	-6.36	5.6	4.3	394	-1.4
Toulon Springs	GW 1	03/08/2016	14.0	7.0	590	4.4	104.2	8.9	6.3	0.8	354.0	10.8	7.5	13.0	14.8	-6.41	5.8	4.7	391	-1.7
Toulon Springs	GW 1	16/08/2016	14.0	7.0	590	4.2	103.4	9.1	6.3	0.8	352.3	10.9	7.5	12.9	14.9	-6.46	5.2	2.7	351	-1.7
Toulon Springs	GW 1	14/09/2016	14.1	7.0	587	3.8	101.6	9.8	6.2	0.9	348.6	11.0	7.5	12.3	14.3	-6.49	5.2	2.5	352	-1.5
Toulon Springs	GW 1	03/10/2016	14.1	7.0	585	4.0	100.4	10.6	6.1	0.8	349.0	11.0	7.5	11.5	13.5	-6.48	5.6	4.9	341	-1.5
Toulon Springs	GW 1	09/11/2016	14.1	7.1	582	4.0	101.2	11.4	6.2	1.0	347.0	11.0	7.5	10.6	13.7	-6.51	5.0	2.9	327	-0.2
Toulon Springs	GW 1	22/11/2016	14.1	7.0	584	4.1	102.3	11.5	6.3	0.9	348.1	11.0	7.5	10.2	13.8	-6.53	4.6	2.2	350	0.2
Toulon Springs	GW 1	16/12/2016	14.0	7.1	589	4.5	103.7	10.4	6.2	1.0	348.7	11.3	8.0	13.6	13.9	-6.47	4.6	2.2	317	-0.6
Toulon Springs	GW 1	21/12/2016	14.1	7.0	588	4.5	101.9	10.6	6.3	0.9	346.6	11.2	8.0	13.3	14.0	-6.51	5.9	3.3	313	-0.8
Toulon Springs	GW 1	04/01/2017	14.0	7.1	586	4.3	100.6	11.2	6.1	0.9	349.6	11.1	7.7	11.9	14.0	-6.49	6.2	3.7	310	-1.1

848

Sample description, chemical composition (mg L^{-1}) and isotopic composition (‰) of borehole samples.

Sample designation	Sample name	Date	Aquifer	T (°C)	pH (pH unit)	EC (µS cm^{-1})	O_2 (mg L^{-1})	Ca^{2+} (mg L^{-1})	Mg^{2+} (mg L^{-1})	Na^{+} (mg L^{-1})	K^{+} (mg L^{-1})	HCO_3^{-} (mg L^{-1})	Cl^{-} (mg L^{-1})	SO_4^{2-} (mg L^{-1})	NO_3^{-} (mg L^{-1})	SiO_2 (mg L^{-1})	$\delta^{18}O_{-H2O}$ (‰)	$\delta^{15}N_{-NO3}^{-}$ (‰)	$\delta^{18}O_{-NO3}^{-}$ (‰)	Balance (%)
Cornille Borehole	B1	05/11/2015	upper Jurassic - Turonian	15.3	6.9	676	2.3	132.8	5.7	7.0	1.8	414.8	13.1	9.2	13.1	15.1	-	7.3	5.0	-0.7
Cornille Borehole	B1	18/09/2017	upper Jurassic - Turonian	17.3	7.1	609	1.2	97.8	21.1	5.2	0.6	395.3	8.9	7.0	1.3	10.6	-	10.3	8.3	0.0
Roussie Borehole	B2	06/11/2015	Turonian - Coniacian	15.0	7.1	590	6.9	118.9	3.2	6.7	1.5	341.6	10.6	7.2	11.2	25.0	-	1.7	1.3	2.4
Roussie Borehole	B2	18/09/2017	Turonian - Coniacian	14.3	7.2	577	6.7	121.2	2.6	6.2	0.4	359.7	9.4	6.3	11.7	24.9	-	2.9	2.9	0.5
P1P Borehole	B3	23/05/2016	Turonian	14.7	7.1	572	1.6	94.5	13.7	6.5	0.7	350.3	10.5	9.6	6.8	15.7	-	5.8	4.7	-1.4
P1P Borehole	B3	20/07/2016	Turonian	15.0	7.1	568	1.9	91.3	13.2	6.2	0.5	345.6	10.6	8.1	6.3	14.8	-	5.5	3.7	-2.3
Trelissac Borehole	B4	18/09/2017	Middle Jurassic	20.8	7.1	562	0.1	85.5	22.1	6.3	0.4	361.4	9.2	7.8	0.0	9.0	-	-	-	0.4

Sample description, nitrogen composition (mg L^{-1}) and isotopic composition (‰) of nitrate potential sources samples.

Sample designation	Sample name	Date	NO_2^{-} (mg L^{-1})	NO_3^{-} (mg L^{-1})	NH_4^{+} (mg L^{-1})	$\delta^{18}O_{-H2O}$ (‰)	$\delta^{15}N_{-NO3}^{-}$ (‰)	$\delta^{18}O_{-NO3}^{-}$ (‰)
Périgueux Rainfall	NS 1	23/05/2016	0.0	1.4	0.6	-4.79	-5.4	61.3
Sewage	NS 2	22/03/2017	0.1	171.8	0.0	-	6.3	-2.9
Sewage	NS 2	19/09/2017	0.1	169.9	0.1	-	6.3	-4.2
Sewage	NS 2	18/11/2017	1.1	179.7	2.3	-	-1.9	-4.8
Ammonium nitrate	NS 3	15/11/2017	-	-	-	-	1.1	23.5
Ammonium nitrate	NS 3	15/05/2016	-	-	-	-	0.9	23.5
Agricultural soil	NS 4	19/09/2017	1.6	0.7	1.3	-	-1.9	0.2
Agricultural soil	NS 4	18/11/2017	1.1	2.2	0.1	-	1.3	2.8
Sewage sludge soil	NS 5	19/09/2017	0.9	0.3	0.5	-	10.9	27.0
Sewage sludge soil	NS 5	18/11/2017	0.5	0.1	0.4	-	33.8	57.5
N_{Tot} soil	NS6	19/09/2017	-	-	-	-	6.8	-
N_{Tot} soil	NS6	18/11/2017	-	-	-	-	6.8	-

856 **References**

857

858 Alexia P., Moussa I., Payre V., Probst A., Probst J.-L., (2015) Flood survey of nitrate
859 behaviour using nitrogen isotope tracing in the critical zone of a French agricultural
860 catchment. Comptes rendus Geoscience 347 (7-8): 328-337.

861

862 Aravena R., Evans M.L., Cherry J.A. (1993) Stable isotopes of oxygen, and nitrogen source
863 identification of nitrate from septic systems. Ground Water 31: 180-186.

864

865 Atkinson T.C., Smoth D.I.., Lavis J.J., Whitaker R.J., (1973) Experiments in tracing
866 underground waters in limestones. Journal of Hydrology 19 : 323-349.

867

868 Bakalowicz M., (2005). Karst groundwater : a challenge for new resources. Hydrogeology
869 Journal 13, 148-160.

870

871 Bateman A.S., Kelly S.D., (2007) Fertilizer nitrogen isotope signatures. Isotopes
872 Environmental Health Studies 43: 237-247.

873

874 Böttcher J., Strebel O., Voerkelius S., Schmidt H.-L. (1990) Using isotope fractionation of
875 nitrate-nitrogen and nitrate-oxygen, for evaluation of microbial denitrification in a sandy
876 aquifer. Journal of Hydrology, 114: 413-424.

877

878 Briand C., Sebilo M., Louvat P., Chesnot T., Vaury V., Schneider M., Plagnes V., (2017)
879 Legacy of contaminant N sources to the NO3- signature in rivers: a combined isotopic (δ^{15}N-
880 NO_3^-, δ^{18}O-NO_3^-, δ^{11}B) and microbiological investigation. Scientific reports 7: 41703.

881

882 Bu H., Song W., Zhang Y., Meng W., (2017) Sources and fate of nitrate in the Haicheng
883 River basin in Northeast China using stable isotope of nitrate. Ecological Engineering 98:
884 105-113.

885

886 Choi W.-J., Lee S.-M., Ro H.-M., Kim K ;-C., Yoo S.-H. (2002) Natural ^{15}N abundances of
887 maize and soil amended with urea and composted pig manure. Plant and Soil 245: 223-232.

888

889 Cholet C., Steinmann M., Charlier J.-B., Denimal S., (2018) Characterizing fluxes of trace
890 metals related to dissolved and suspended matter during a storm event: application to a karst
891 aquifer using trace metal and rare earth elements as provenance indicators. Hydrogeology
892 Journal, https://doi.org/10.1007/s10040-018-1859-2.

893

894 Cravotta C. (2002) Use of stable isotopes of carbon, nitrogen, and sulfur to identify sources
895 of nitrogen in surface waters in the lower Susquehanna River Basin, Pennsylvania. (U.S.
896 G.P.O., 2002).

897

898 De Roos A.J., Ward M.H., Lynch C.F., Cantor K.O., (2003) Nitrate in public water systems
899 and the risk of colon and rectum cancers. Epidemiology 14: 640-649.

900

901 Derse E., Knee K.L., Wankel S.D., Kendall C., Berg Jr., D.J., Paytan A., (2007) Identifying
902 sources of nitrogen to Hanalei Bay, Kauai, utilizing the nitrogen isotope signature of
903 microalgae. Environmental Science Technology 41: 5217-5223.

904

905 Eller K., Katz B., (2017) Nitrogen Source Inventory and Loading Tool: An integrated
906 approach toward restoration of water quality impaired karst springs. Journal of
907 Environmental Management 196: 702-709.
908
909 El Gaouzi F.J., Sebilo M., Ribstein P., Plagnes V., Boeckx P., Xue D., Derenne S.,
910 Zakeossian M., (2013) Using $\delta^{15}N$ and $\delta^{18}O$ values to identify sources of nitrate in karstic
911 springs in the Paris basin (France). Applied Geochemistry 35: 230-243.
912
913 Ford D., Willians P., (2007) Hydrogeology and geomorphology. 2nd ed. Chichester Wiley;
914 2007.
915
916 Geyer T., Birk S., Licha T., Liedl R., Sauter M., (2007) Multitracer test approach to
917 characterize reactive transport in karst aquifers. Ground Water 45, 36-45.
918
919 Goldscheider N., Chen Z., Auler A., Bakalowicz M., Broda S., Drew D., Hartman J., Jiang
920 G., Moosdorf N., Stevanovic Z., Veni G. (2020) Global distribution of carbonate rocks and
921 karst water resources. Hydrogelogy Journal 28: 1661-1677.
922
923 Heaton T.H.E., Stuart M.E., Sapiano L., Sultana M.M., (2012) An isotope study of the
924 sources of nitrate in Malta's groundwater. Journal of Hydrology 414-415: 244-254.
925
926 Heaton T.H.E., Trick J.C., Williams G.M., (2005) Isotope and dissolved gas evidence for
927 nitrogen attenuation in landfill leachate dispersing into a chalk aquifer. Applied
928 Geochemistry 20: 933-945.
929

930 Högberg P., (1997) Transley review n°95: 15N natural abundance in soil-plant systems. New
931 Phytologist 137: 179-203.
932
933 Huebsch M., Fenton O., Horan B., Hennessy D., Richards K.G., Jordan P., Goldscheider N.,
934 Butscher C., Blum P., (2014) Mobilisation or dilution ? Nitrate responses of karst springs to
935 high rainfall events. Hydrology and Earth System Sciences 18 : 4423-4435.
936
937 Huneau F., Jaunat K., Kavouri K., Plagnes V., Rey F., Dörfliger N., (2013) Intrinsic
938 vulnerability mapping for small moutainous karst aquifers, implementation of the new
939 PapRIKa method to Western Pyrenees (France). Engineering Geology 161: 81-93.
940
941 Katz B.G., Sepulveda A.A., Verdi R.J., (2009) Estimating nitrogen loading to groundwater
942 and assessing vulnerability to nitrate contamination in a large karstic spring basin, Florida.
943 Journal of the American Water Resources Association 45 (3) : 607-627.
944
945 Kendall C., McDonnell J.J. (1998) Tracing nitrogen sources and cycling in catchments. In:
946 Kendall C., McDonnell J.J., (Eds), Isotope Tracers in Catchment Hydrology: 519-576.
947
948 Kendall C., Elliott E.M., Wankel S.D., (2007) Tracing anthropogenic inputs of nitrogen to
949 ecosystems. In: Michener R., Lajtha K., (Eds). Stable Isotopes in Ecology and Environmental
950 Science. Blackwell Publishing: 375-449.
951
952 Labat D., Mangin A., (2015) Transfer function approach for artificial tracer test interpretation
953 in karstic systems. Journal of Hydrology 529: 866-871.
954

955 Lastennet R., Huneau F., Denis A., (2004) Geochemical characterization of complex
956 multilayer karstic systems. Springs of Périgueux, France. Proceedings of the international
957 Transdisciplinary Conference on Development and Conservation of Karst Regions, Hanoi,
958 Vietnam. 132-135.
959
960 Liu C.Q., Li S.L., Lang Y.C., Xiao H.Y., (2006) Using 15N and 18O values to identify
961 nitrate sources in karst ground water, Guiyang, southwest China. Environmental Science
962 technology 40: 6928-6933.
963
964 Li S.-L., Liu C.-Q., Lang Y.-C., Zhao Z.-Q., Zhou Z.-H. (2010) Tracing the sources of nitrate
965 in karstic groundwater in Zunyi, Southwest China: a combined nitrogen isotope and water
966 chemistry approach. Environmental Earth Sciences 60 (7): 1415-1423.
967
968 Li S.-L., Liu C.-Q., Li J., Xue Z., Guan J., Lang Y., Ding H., Li L., (2013) Evaluation of
969 nitrate source in surface water of westhern China based on stable isotopes. Environmental
970 Earth Sciences 68, 219-228.
971
972 Li Z., Walters W., Hasting M., Zhang Y., Song L., Liu D., Zhang W., Pan Y., Fu P., Fang Y.
973 (2019) Nitrate Isotopic Composition in Precipitation at a Chinese Megacity: Seasonal
974 Variations, Atmospheric Processes, and Implications for Sources. Earth and Space Science 6,
975 2200-2213.
976
977 Lombardo Associates (2011) Onsite sewage Treatment and Disposal and Management
978 Options (Newton, MA).
979

Lorette G. (2019) Fonctionnement et vulnérabilité d'un système karstique multicouche à partir d'une approche multi-traceurs et d'un suivi haute résolution. University of Bordeaux, France PhD. (291p). DOI: 10.13140/RG.2.2.21668.01921

Lorette G., Lastennet R., Peyraube N., Denis A., (2017) Examining the functioning of a multilayer karst aquifer. The case of Toulon springs. In: Renard, P., Bertrand, C. (Eds.), EuroKarst 2016, Neuchâtel, Advances in Karst Science. Springer International Publishing, Cham, pp. 363–370. https://doi.org/10.1007/978-3-319-45465-8_35

Lorette G., Lastennet R., Peyraube N., Denis A., (2018) Groundwater-flow characterization in a multilayered karst aquifer on the edge of a sedimentary basin in western France. Journal of Hydrology 566: 137-149.

Lorette G., Peyraube N., Lastennet R., Denis A., Sabidussi J., Fournier M., Viennet D., Gonand J., Villanueva J.D. (2020) Tracing water perturbation using NO_3^-, doc, particles size determination, and bacteria: A method development for karst aquifer water quality hazard assessment. Sciences of the Total Environnement 725, 138512.

Lorette G., Viennet D., Labat D., Massei N., Fournier M., Sebilo M., Crancon P. (2021) Mixing processes of autogenic and allogenic waters in a large karst aquifer on the edge of a sedimentary basin (Causses du Quercy, France). Journal of Hydrology 593, 125859.

Luz B., Barkman E., (2011) The isotopic composition of atmospheric oxygen. Global Biogeochemical Cycles 25: GB3001.

1005 Mahler B.J., Bourgeais R., (2013) Dissolved oxygen fluctuations in karst spring flow and
1006 implications for endemic species: Barton Springs, Edwards aquifer, Texas, USA. Journal of
1007 Hydrology 505, 291-298.
1008
1009 Mahler B.J., Musgrove M., Wong C.I., Sample T.L., (2011) Recent (2008-10) water quality
1010 in the Burton Springs segment of the Edwards aquifer and its contributing zone, Central
1011 Texas, with emphasis on factors affecting nutrients and bacteria. U.S. Geological Survey
1012 Scientific Investigations Report 2011-5139, 66 p.
1013
1014 Malher B.J., Valdes D., Musgrove M., Massei N., (2008) Nutrient dynamics as indicators of
1015 karst precesses : Comparison of the Chalk aquifer (Normandy, France) and the Edwards
1016 aquifer (Texas, France). Journal of Contaminant Hydrology 98 : 36-49.
1017
1018 Marín A., Andreo B., Mudarra M., (2015) Vulnerability mapping and protection zoning of
1019 karst springs. Validation by multitracers tests. Science of The Total Environment 532: 435-
1020 446.
1021
1022 Mariotti, A., (1982) Apports de la géochimie isotopique à la connaissance du cycle de
1023 l'azote. Ph.D. Thesis. Univ. Pierre et Marie Curie, Paris 6, France.
1024
1025 Mariotti A., Germon J.C., Hubert P., Kaiser P., Letolle R., Tardieux A., Tardieux P., (1981)
1026 Experimental determination of nitrogen kinectiv isotope fractionation: some principles;
1027 illustration for the denitrification and nitrification processes. Plant Soil 62 : 413-430.
1028

1029 Mayer B., Bollwerk S.M., Mansfeldt T., Hütter B., Veizer J. (2001) The oxygen isotope
1030 composition of nitrate generated by nitrification in acid forest floors. Geochimica et
1031 Cosmochimica Acta 65, 2743‑2756.
1032
1033 Mayer B., Boyer W.E., Goodale C., JAworski N.A., Van Breemen N., Howarth R.W.,
1034 Seitzinger S., Billen G., Lajtha K., Naderlhoffer K., Van Dam D., Getling L.J., Nosal M.,
1035 Paustian K., (2002) Sources of nitrate in rivers draining sixteen watersheds in the
1036 northeastern U.S.: isotopic constraints. Biogeochemistry 57 (58): 171-197.
1037
1038 McAlvin M., Altabet M., (2005) Chemical conversion of nitrate and nitrite to nitrous oxide
1039 for nitrogen and oxygen isotopic analysis in Freshwater and seawater. Analytical chemistry
1040 77: 5589-5595.
1041
1042 Mengis M., Schif S.L., Harris M., English M., Aravena R., Elgood R., MacLean A., (1999)
1043 Multiple geochemical and isotopic approaches for assessing groundwater NO_3^- elimination in
1044 a Riparian zone. Ground Water 37, 448-457.
1045
1046 Mudarra M., Andreo B., Marín A., Vadillo I., Barberá J., (2014) Combined use of natural and
1047 artificial tracers to determine the hydrogeological functioning of a karst aquifer : the
1048 Villanueva del Rosario system (Andalusia, southern Spain) Hydrogeology Journal 22 : 1027-
1049 1039.
1050
1051 Musgrove M., Fahlquist L., Stanton G.P., Houston N.A., Lindgren R.J., (2011)
1052 Hydrogeology, chemical characteristics, and water sources and pathways in the zone of

1053 contribution of a public-supply well in San Antonio, Texas. U.S. Geological survey Scientific
1054 Investigations Report 2011-5146, 194 p.
1055
1056 Musgrove M., Opsahl S., Mahler B., herrington C., Sample T., Banta J., (2016) Source,
1057 variability and transformation of nitrate in a regional karst aquifer: Edwards aquifer, central
1058 Texas. Science of the Total Environment 568: 457-469.
1059
1060 Nolan B.T., Stone J.D., (2000) Nutrients in ground waters of the coterminous United States,
1061 1992-1995. Environmental Science and Technology 34: 1156-1165.
1062
1063 Nômmik H., Pluth D.J., Larsson K., Mahendrappa M.K., (1994) Isotopic fractionation
1064 accompanying fertilizer nitrogen transformations in soil and trees of a Scots pine ecosystem.
1065 Plant Soil 159: 169-182.
1066
1067 Opsahl S., Musgrove M., Slattery R., (2017) New insights into nitrate dynamics in a karst
1068 groundwater system gained from in situ high-frequency optical sensor measurements.
1069
1070 Perrin J., Jeannin P.-Y., Cornaton F., (2007) The role of tributary mixing in chemical
1071 variations at a karst spring, Milandre, Switzerland. Journal of Hydrology 332, 152-173.
1072
1073 Pu J., Yuan D., He Q., Wang Z., Hu Z., Gou P., (2011) High-resolution monitoring of nitrate
1074 variations in a typical subterranean karst stream, Chongqing, China. Environmental Earth
1075 Sciences 64 : 1985-1993.
1076

1077 Puig R., Folch A., Mencio A., Soler A., Mas-Pla J., (2013) Multi-isotopic study (^{15}N, ^{34}S,
1078 ^{18}O, ^{13}C) to identify processes affecting nitrate and sulfate in response to local and regional
1079 groundwater mixing in a large-scale flow system. Applied Geochemistry 32 : 129-141.
1080
1081 Pronk M., Goldscheider N., Zopfi J., Zwahlen F., (2009) Percolation and particle transport in
1082 the unsaturated zone of a karst aquifer. Ground Water 47 : 361-369.
1083
1084 Rey F., Huneau F., Riss J., Prétou F., (2006) Use of multiple sources statistics to delineate the
1085 hydrogeological functioning of carbonated systems (example of the Western Pyrenees,
1086 France). International Association for Mathematical Geology, XIth International Congress,
1087 September 3-8 2006, Liège (Belgium).
1088
1089 Rowden R., Liu H., Libra R., (2001) results from big spring basin water quality monitoring
1090 and demonstration projects, Iowa, USA. Hydrogeology Journal 9 : 487-497.
1091
1092 Sebilo M., (2003) Utilisation du traçage isotopique naturel pour caractériser et quantifier les
1093 processus de nitrification et de dénitrification à l'échelle du réseau hydrographique de la
1094 Seine. Ph.D. Thesis. Univ. Pierre et Marie Curie, Paris 6, France.
1095
1096 Sebilo M., Mayer B., Nicolardot B., Pinay G., Mariotti A. (2013) Long-term fate of nitrate
1097 fertilizer in agricultural soils. Proceedings of The National Academy of Sciences.
1098 DOI :10.7079/pnas.1305372110
1099

1100 Sebilo M., Aloisi G., Mayer B., Perrin E., Vaury V., Aurélie M., Laverman A. (2019)
1101 Controls on the isotopic composition of nitrite ($\delta^{15}N$ and $\delta^{18}O$) during denitrification in
1102 freshwater sediments. Scientific reports 9:19206 https://doi.org/10.1038/s41598-019-54014-3
1103
1104 Schwientek M., Osenbrück K., Fleisher M., (2013) Investigating hydrological drivers of
1105 nitrate export dynamics in two agricultural catchments in Germany using high-frequency data
1106 series. Environmental Earth Sciences 69: 381-393.
1107
1108 Semaoune P., Sebilo M., Templier J., Derenne S., (2012) Is there any isotopic fractionation
1109 of nitrate associated with diffusion and advection? Environmental Chemistry 9: 158-162.
1110
1111 Singleton M.J., Esser B.K., Moran J.E., Hudson G.B., McNab W.W., Harter T., (2007)
1112 Saturated zone denitrification: potential for natural attenuation of nitrate contamination in
1113 shallow groundwater under dairy operations. Environmental Science Technology 41: 759-
1114 765.
1115
1116 Sivelle V., Labat D., (2019) Short-term variations in tracer-test responses in a highly
1117 karstified watershed. Hydrogeology Journal. DOI: 10.1007/s10040-019-01968-3
1118
1119 Stevanović Z. (2015) Karst Aquifers - Characterization and Engineering, Professional
1120 Practice in Earth Sciences. Springer International Publishing. https://doi.org/10.1007/978-3-
1121 319-12850-4
1122
1123 Stevanović Z. (2019) Karst waters in potable water supply: a global scale overview.
1124 Environmental Earth Sciences 78, 662. https://doi.org/10.1007/s12665-019-8670-9

1125

1126 Stueber A.M., Criss R.E., (2005) – Origin and transport of dissolved chemicals in a karst
1127 watershed, southwestern Illinois. Journal of American Water Resources Association 41 : 267-
1128 290.

1129

1130 Valiente N., Gil-Márquez J.M., Gómez-Alday J.J, Adreo B. (2020) Unravelling groundwater
1131 functioning and nitrate attenuation in evaporitic karst systems from southern Spain: an
1132 isotopic approach. Applied Geochemistry

1133

1134 Vitoria L., Otero N., Soler A., Canals A., (2004) Fertilizer characterization: isotopic data (N,
1135 S, O, C, and Sr). Environmental Science Technology 38: 3254-3262.

1136

1137 Von Stempel C. (1972) Etude des ressources en eau de la région de Périgueux (Dordogne.
1138 Thèse de Doctorat en Sciences naturelles, Université de Bordeaux I, 235 p.

1139

1140 Wang Z.J., Li S.-L., Yue F.-J., Q C.-Q., Buckerfield S., Zeng J. (2020) Rainfall driven nitrate
1141 transport in agricultural karst surface river system : Inseight from high resolution
1142 hydrochemistry and nitrate isotopes. Agriculture, ecosystems & Environment 291: 106787.

1143

1144 Ward M.H., DeKok T., Levallois P., Brender J., Gulis G., Nolan B.T., VanDerslice J., (2005)
1145 Drinking water nitrate and health – recent findings and research needs. Environmental Health
1146 Perspectives 115: 1607-1614.

1147

1148 White W.B., (1988) Geomorphology and Hydrology of Karst terrains. Oxford University
1149 press, New York, 464 p.

1150

1151 Xue D., Botte J., De Baets B., Accoe F., Nestler A., Taylor P., Cleemput O., Berglund M.,
1152 Boeckx P., (2009) Present limitations and future prospects of stable isotope methods for
1153 nitrate source identification in surface and groundwater. Water Research 43: 1159-1170.

1154

1155 Yang P., Li Y., groves C., Hong A., (2019) Coupled hydrogeochemical evauation of a
1156 vulnerable karst aquifer impacted by septov effluent in a protected natural area. Science of
1157 the Total Environment 658: 1475-1484.

1158

1159 Yue F.-J., Li S.-L., Liu C.-Q., Zhao Z.-Q., Ding H. (2017) Tracing nitrate sources with dual
1160 isotopes and long term monitoring of nitrogen species in the Yellow River, China. Scientific
1161 Report 7: 8537. DOI:10.1038/s41598-017-08756-7

1162

1163 Yue F.-J., Waldron S., Li S.-L., Wang Z.-J., Zeng J., Xu S., Zhang Z.-C., Oliver D., (2019)
1164 Land use interacts with changes in catchment hydrology to generate chronic nitrate pollution
1165 in karst waters and strong seasonality in excess nitrate export. Science of the Total
1166 Environment 696: 134062.